Published by Institute of Physics Publishing for SISSA/ISAS
Received: *April 04, 2002*
Revised: *May 16, 2002*
Accepted: *May 16, 2002*

Cross section of isolated prompt photons in hadron-hadron collisions

Stefano Catani*
Theory Division, CERN, CH-1211 Geneva 23, Switzerland
E-mail: stefano.catani@cern.ch

Michel Fontannaz
Laboratoire de Physique Théorique LPT, Université de Paris XI
F-91405 Orsay Cedex, France
E-mail: Michel.Fontannaz@th.u-psud.fr

Jean-Philippe Guillet and Eric Pilon
Laboratoire d'Annecy-Le-Vieux de Physique Théorique LAPTH
F-74941 Annecy-le-Vieux, France
E-mail: guillet@lapp.in2p3.fr, pilon@lapp.in2p3.fr

Abstract: We consider the production of isolated prompt photons in hadronic collisions. We present a general discussion in QCD perturbation theory of the isolation criterion used by hadron collider experiments. The isolation criterion is implemented in a computer programme of the Monte Carlo type, which evaluates the production cross section at next-to-leading order accuracy in perturbative QCD. The calculation includes both the direct and the fragmentation components of the cross section, without any approximation of the dependence on the radius R of the isolation cone. We examine the scale dependence of the isolated cross section, the sensitivity of the cross section to the values of the isolation parameters, and we provide a quantitative comparison between the full R dependence and its small-R approximation.

Keywords: NLO Computations, Hadronic Colliders, QCD.

*On leave of absence from INFN, Sezione di Firenze, Florence, Italy.

JHEP05(2002)028

Contents

1. Introduction

The production of prompt photons with large transverse momenta p_T at hadronic colliders has been the subject of a continuing effort, both experimentally [1]–[6] and theoretically [7]–[12], during the last fifteen years. The expression "prompt photons" means that these photons do not come from the decay of hadrons, such as π^0, η, etc. produced at large transverse momenta. Prompt-photon production is an interesting observatory of the short-distance dynamics of quarks and gluons by using a hard colourless probe. It is complementary to the electroweak processes of Deep Inelastic Scattering and Drell-Yan pair production, and to pure QCD processes such as inclusive production of jets or heavy flavours. One of the main motivations of its study is its sensitivity to the gluon density inside the colliding hadrons [13]. Indeed the gluon distribution function is involved already at the lowest order (LO) in the strong coupling α_s through the "QCD Compton" subprocess

$qg \to \gamma q$, which dominates at fixed-target energies. Moreover the point-like coupling of the photon to quarks in principle makes the process of prompt-photon production ideally free from the uncertainties inherent in jet reconstruction (as in the case of jet production) or in fragmentation of partons into hadrons (as in inclusive hadron production).

In fact, the latter feature is not as ideal as initially thought, because prompt photons can be produced according to two possible mechanisms, one of them being a fragmentation mechanism. Whereas the contribution from fragmentation remains small (less than 10%) at fixed-target energies, it becomes dominant in inclusive prompt-photon production at colliders. This was already true at the CERN $Sp\bar{p}S$, at least in the lower range of the p_T spectrum for the UA1 and UA2 experiments at the centre-of-mass (c.m.) energy $\sqrt{S} = 630\,\mathrm{GeV}$. It is true at the Tevatron ($\sqrt{S} \sim 2\,\mathrm{TeV}$), and will remain true at the LHC ($\sqrt{S} = 14\,\mathrm{TeV}$), since this dominance increases with $\sqrt{S}$.

To be precise, the collider experiments at the Tevatron and at the forthcoming LHC do not perform *inclusive* photon measurements. The background of secondary photons coming from the decays of π^0, η, etc. overwhelms the signal by several orders of magnitude. To reject this background, the experimental selection of prompt photons requires *isolation* cuts. The isolation criterion used by collider experiments is schematically as follows. A photon is said to be isolated if, in a cone of radius R in rapidity and azimuthal angle around the photon direction, the amount of deposited hadronic transverse energy E_T^{had} is smaller than some value $E_{T\,\max}$ chosen by the experiment:

$$E_T^{\mathrm{had}} \leq E_{T\,\max}\,, \qquad \text{inside } (y - y_\gamma)^2 + (\phi - \phi_\gamma)^2 \leq R^2\,. \tag{1.1}$$

In addition to the rejection of the background of secondary photons, the isolation cuts also affect the prompt-photon cross section itself, in particular by reducing the effect of fragmentation.

Hadronic production of isolated prompt photons is not relevant only to QCD studies. The LHC experiments, ATLAS and CMS, will search neutral Higgs bosons in the mass range 80–140 GeV through the decay channel $H \to \gamma\gamma$ [14]. The production of pairs of isolated prompt photons with a large invariant mass is the so-called irreducible background to this search. Therefore, a quantitative understanding of this background is relevant to reliably estimate the expected significance $S/\sqrt{B}$ (S and B being the number of expected Higgs boson events and background events, respectively). This provides another important motivation for studying isolation in prompt-photon reactions.

Various issues on isolation of photons based on the above criterion[1] have already been discussed in the literature [8]–[12]. The aim of the present article is to provide a detailed QCD study of the isolation criterion (1.1), and to present a complete (without any small-R approximation) calculation at next-to-leading order (NLO) accuracy in QCD perturbation theory.

[1] Other isolation criteria have also been discussed. We mention, in particular, the alternative criterion proposed in ref. [15] and studied in ref. [16] and in ref. [17, section 6.3]. The related topic of isolated photons produced in e^+e^- collisions has also been abundantly discussed. A variant of (1.1) suitable for e^+e^- was studied in [18] and revisited in [19, 20, 21]. A different criterion [22] for isolated photons in jets has also been applied in measurements of the LEP experiments.

The first theoretical question raised by the implementation of isolation is an issue of principle. Since the production of isolated photons, and more generally of any isolated particle, is no longer an inclusive process, one may question the validity of the factorization theorem of collinear singularities that is established in the inclusive case [19]. In the case of e^+e^- annihilation into an isolated prompt photon plus hadrons, this issue was examined in ref. [21]. It was shown that factorization still holds in terms of the same fragmentation functions as appear in the inclusive case, whereas the dependence on the isolation parameters is consistently taken into account by the short-distance partonic cross section. The case of hadronic collisions is more involved, since factorization is complicated by the presence of initial-state collinear singularities in the perturbative calculation. In this paper we extend the treament of ref. [21] to hadronic collisions, we consider the isolation criterion (1.1) and some variants of it, and we discuss and prove factorization to any order in QCD perturbation theory.

The evaluation of NLO QCD corrections to the inclusive production of a single isolated prompt photon in hadron-hadron collisions was considered in refs. [9, 11]. The authors of ref. [9] computed the NLO corrections to direct photon production, without including those to the fragmentation mechanism. The NLO calculation of ref. [11] includes both the direct and fragmentation mechanisms, and it uses the small-cone approximation $R \ll 1$. More precisely, the approach of ref. [11] is based on an analytical treatment of isolation in which the transverse energies, rapidities and azimuthal angles in eq. (1.1) are replaced by energies and relative angles defined in the hadronic c.m. frame. This substitution of variables has no effect in the small-cone approximation. To go beyond the small-cone approximation, in this paper we carry on our study in terms of the variables η, ϕ and E_T involved in the criterion (1.1). Since these variables are invariant under longitudinal boosts along the direction of the beam axis, the criterion in eq. (1.1) is current practice in experiments at high-energy hadron colliders. We perform a complete NLO calculation: it includes both the direct and fragmentation contributions without any small-cone approximation. Our approch is based on a combined analytical and numerical treatment, and it can be used to implement different variants of the isolation criterion (1.1).

This paper is organized as follows. In section 2, we recall the two production mechanisms (direct and fragmentation) of a prompt photon. In section 3 we present a brief pedagogical discussion on non-isolated prompt photons: using the collinear approximation, we derive analytic expressions for the direct and fragmentation contributions to the NLO cross section. The general factorization issues that are raised in the case of isolated particle hadroproduction are discussed in section 4. In section 5, we show how the implementation of isolation affects the analytic expressions of section 3 in the limit of small values of the radius R of the isolation cone. To go beyond the small-R approximation, we implement the NLO calculation of the isolated-photon cross section in a computer programme of the Monte Carlo type. The computer programme, which enables us to evaluate the full R dependence of the cross section, is described in section 6, where we also present some numerical results and comparisons with the small-R approximation. In section 7 we summarize our results and we conclude with some remarks on questions left open when the cone radius R becomes small or the isolation condition becomes very tight (when $E_{T\,\max}$ becomes small).

JHEP05(2002)028

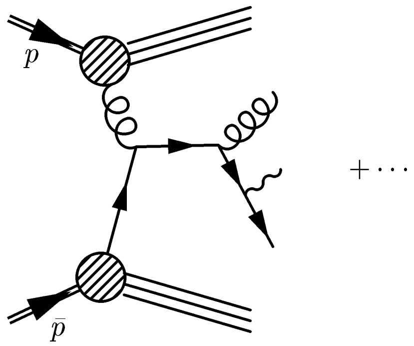

Diagram a

2. Mechanisms of prompt-photon production

As mentioned in section 1, schematically, a high-p_T prompt photon can be produced by two possible mechanisms: either it takes part directly in the hard subprocess, or it results from the collinear fragmentation of a parton that is itself produced with a large transverse momentum. From a topological point of view, when a "direct" photon is produced, it is most probable that it will be separated from the hadronic environment, whereas a photon "from fragmentation" is most probably accompanied by hadrons, except when the photon carries away most of the momentum of the fragmenting parton. These fragmentation configurations are rare and atypical, and they are precisely those that are not suppressed by the isolation criterion.

The LO contribution to direct prompt-photon production is given by the Born-level processes $q\bar{q} \to \gamma g$ and q (or $\bar{q}$) $g \to \gamma q$ (or $\bar{q}$). The computation of the NLO contributions yields $\mathcal{O}(\alpha_s)$ corrections coming from the subprocesses $q\bar{q} \to \gamma gg$, gq (or $\bar{q}$) $\to \gamma gq$ (or $\bar{q}$) and from the virtual corrections to the Born-level processes.

The calculation of these higher order corrections also yields the LO contribution of the fragmentation type (sometimes called "bremsstrahlung contribution"), in which the photon comes from the collinear fragmentation of a hard parton produced in a short-distance subprocess (see, for instance, Diagram a). This contribution appears in the following way. A final-state quark-photon collinear singularity occurs in the calculation of the contribution from the subprocess $gq \to \gamma\gamma q$. At higher orders, final-state multiple collinear singularities appear in any subprocess where a high-p_T parton (quark or gluon) undergoes a cascade of successive collinear splittings ending up with a quark-photon splitting. These singularities are factorized to all orders in α_s and absorbed into quark and gluon fragmentation functions of the photon, $D_q^\gamma(z, M_F^2)$ and $D_g^\gamma(z, M_F^2)$, defined in a certain factorization scheme at a factorization scale M_F chosen to be of the order of the hard scale of the process. When the fragmentation scale M_F is large with respect to $\sim 1\,\text{GeV}$, these functions behave roughly as $\alpha/\alpha_s(M_F^2)$, so that these contributions are of the same order in α_s as the Born-level terms in the direct mechanism. Moreover, because of the high value of the gluon parton densities at small momentum fraction x, the gq (or $\bar{q}$) initiated contribution producing

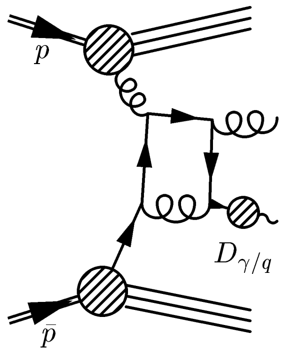

Diagram b

$+\cdots+$

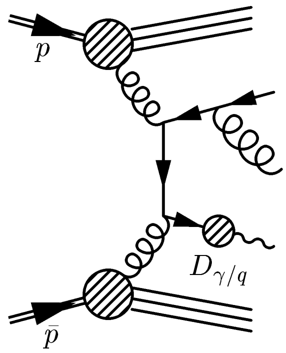

Diagram c

$+\cdots$

one photon from fragmentation even dominates the inclusive production rate in the lower range of the photon p_T-spectrum at the Tevatron, and this will be even more true at the LHC. The calculation of the NLO corrections to the fragmentation contribution (see, for instance, Diagrams b and c) is thus required for a reliable and consistent treatment of prompt-photon production at this accuracy.

In this paper, we call "direct" the contribution given by the Born term plus the part of the higher-order corrections from which final-state collinear singularities have been subtracted according to the $\overline{MS}$ factorization scheme. The remaining part is called "fragmentation" contribution, and involves the fragmentation function of a parton into a photon as defined in the $\overline{MS}$ factorization scheme. In our numerical calculations, we use the fragmentation functions of ref. [23].

Note, however, that the above distinction between the two mechanisms has no direct physical meaning beyond LO. From a theoretical point of view, the distinction is defined by an arbitrary choice. It follows from the necessity of factorizing the final-state collinear singularities and absorbing them into the fragmentation functions. This factorization requires the introduction of an arbitrary fragmentation scale M_F, which is an unphysical parameter. More generally, it relies on an arbitrary choice of the factorization scheme, which defines the finite part of the higher-order corrections that is absorbed in the fragmentation functions together with the singularities; the remaining finite part is then included in the higher-order contributions to the partonic cross sections. The dependence on this arbitrariness, and in particular on M_F, cancels only in the sum of the direct and fragmentation contributions, so only this sum is a physical observable. In particular, any experimental identification of direct and fragmentation contributions based on topological grounds does not match the "theoretical identification" used throughout this paper.

3. Inclusive cross section

We start the discussion by considering the inclusive cross section for the production of a non-isolated photon with momentum p_γ. The transverse momentum and the rapidity of the photon are denoted by $p_{T\gamma}$ and y_γ (since the photon is massless, $y_\gamma = \eta_\gamma$ where

η_γ is the pseudorapidity), respectively. The hadronic cross section $d\sigma/dp_{T\,\gamma}dy_\gamma$, which we denote by $\sigma(p_\gamma)$, is given by the sum of the "fragmentation" and "direct" contributions. It can be written, in shorthand, as

$$\sigma(p_\gamma) = \sum_a \int_0^1 \frac{dz}{z}\, \widehat{\sigma}^a \left(\frac{p_\gamma}{z}; \mu, M, M_F\right) D_a^\gamma(z; M_F) + \widehat{\sigma}^\gamma(p_\gamma; \mu, M, M_F)\,, \tag{3.1}$$

where $\widehat{\sigma}^a$ and $\widehat{\sigma}^\gamma$ are the corresponding "partonic" cross sections. The contribution $\widehat{\sigma}^a$ describes the production of a parton a ($a = q, \bar{q}, g$) in the hard collision, and D_a^γ is the fragmentation function of the parton a into a photon. The direct contribution $\widehat{\sigma}^\gamma$ does not contain any fragmentation function; it corresponds to the point-like coupling of the large-p_T photon to a quark produced in the hard subprocess. Note that $\widehat{\sigma}^a$ and $\widehat{\sigma}^\gamma$ are not true partonic cross sections, since they include the convolution with the parton distributions of the colliding hadrons.

The cross sections $\widehat{\sigma}^\gamma$ and $\widehat{\sigma}^a$ are known up to NLO in α_s:

$$\widehat{\sigma}^\gamma(p; \mu, M, M_F) = \left(\frac{\alpha_s(\mu)}{\pi}\right) \sigma_{\text{Born}}^\gamma(p; M) + \left(\frac{\alpha_s(\mu)}{\pi}\right)^2 \sigma_{\text{HO}}^\gamma(p; \mu, M, M_F)\,, \tag{3.2}$$

$$\widehat{\sigma}^a(p; \mu, M, M_F) = \left(\frac{\alpha_s(\mu)}{\pi}\right)^2 \sigma_{\text{Born}}^a(p; M) + \left(\frac{\alpha_s(\mu)}{\pi}\right)^3 \sigma_{\text{HO}}^a(p; \mu, M, M_F)\,. \tag{3.3}$$

The expressions of σ_{HO} (and σ_{Born}) for the direct and fragmentation contributions can be found in refs. [7, 11] and ref. [24] respectively. They depend on the renormalization scale μ, on the factorization scale M of the initial-state parton distributions and on the factorization scale M_F of the photon fragmentation function. These results have been the starting point of the prompt-photon phenomenology of the last fifteen years [7]. More recently, expressions involving resummation of logarithmic terms that are large at the phase-space boundary also became available [25]–[30].

To better understand the differences between the inclusive cross section and the isolated cross section, we need a more detailed expression of $\sigma(p_\gamma)$ in eq. (3.1). Let us first consider the fragmentation contribution in the Born approximation:

$$\begin{aligned} d\sigma_{\text{Born}}^{\text{brems}}[A + B \to \gamma + jet + X] = \frac{1}{8\pi S^2} \sum_{\substack{i,j\\a,b}} \int \frac{G_{i/A}(x_1, M)}{x_1} \frac{G_{j/B}(x_2, M)}{x_2} \times \\ \times |\overline{\mathcal{M}}_B[i + j \to a + b]|^2 D_a^\gamma(z, M_F) \times \\ \times \Theta\left(z - z_{\min}\right)\; dz\; d\eta_b\; d\eta_a\; p_{T\,a}\; dp_{T\,a}\,. \end{aligned} \tag{3.4}$$

Here we are considering the photon-jet double inclusive cross section. The photon has transverse momentum $p_{T\,\gamma} = z\,p_{T\,a}$ and rapidity $\eta_\gamma = \eta_a$. The jet recoiling against the photon, here the parton b, has rapidity $\eta_{jet} = \eta_b$. $|\overline{\mathcal{M}}_B|^2$ is the matrix element squared of the Born subprocess, averaged (summed) over initial-state (final-state) spins and colours. $G_{i/A}(x_1, M)$ and $G_{j/B}(x_2, M)$ are the parton distribution functions of the incoming hadrons, with $x_{1,2}$ given in the hadronic c.m. frame by

$$x_{\frac{1}{2}} = \frac{p_{T\,a}}{\sqrt{S}}\; \left(e^{\pm\eta_a} + e^{\pm\eta_b}\right), \tag{3.5}$$

where transverse momenta, rapidities and the hadronic energy $\sqrt{S}$ are defined in the c.m. frame. We rewrite (3.4) in a more compact form:

$$d\sigma^{\rm brems}_{\rm Born}[A+B\to\gamma+jet+X] = 2\pi\left(\frac{\alpha_s(\mu)}{\pi}\right)^2\sum_{a,b}\int_{z_{\min}}^1 D_a^\gamma(z,M_F)\;dz\;\times \\ \times\int E_a\frac{d\widehat{\sigma}_{\rm Born}[A+B\to a+b+X]}{d\vec{p}_a\;d\eta_b}\;d\eta_b\;d\eta_a\;p_{T\,a}\;dp_{T\,a}\,, \tag{3.6}$$

where $z_{\min}$ is given by

$$z_{\min} = \max\left\{\frac{p_{T\,\gamma}}{\sqrt{S}}\left(e^{\pm\eta_\gamma}+e^{\pm\eta_b}\right)\right\}. \tag{3.7}$$

We can write a similar expression for the higher-order (HO) corrections to the fragmentation contribution:

$$\begin{aligned} d\sigma^{\rm brems}_{\rm HO}&[A+B\to\gamma+jet+x] = \\ &= 2\pi\left(\frac{\alpha_s(\mu)}{\pi}\right)^3\sum_a\int E_a\frac{d\widehat{\sigma}_{\rm HO}[A+B\to a+jet+X]}{d\vec{p}_a\;d\eta_{jet}}\;\times \\ &\qquad\times\;D_a^\gamma(z,M_F)\;dz\;d\eta_{jet}\;d\eta_a\;p_{T\,a}\;dp_{T\,a} \\ &= 2\pi\left(\frac{\alpha_s(\mu)}{\pi}\right)^3\sum_{a,b,i}\int_{z_{\min}}^1 dz\;D_i^\gamma(z,M_F)\int_{z_{\min}/z}^1 dx\;P_{ia}(x)\;\ln\left(\frac{p_{T\gamma}}{M_F}\right)\times \\ &\qquad\times\;E_a\frac{d\widehat{\sigma}_{\rm Born}[A+B\to a+b+X]}{d\vec{p}_a\;d\eta_b}\;d\eta_b\;d\eta_a\;p_{T\,a}\;dp_{T\,a}\;+ \\ &\quad+\;2\pi\left(\frac{\alpha_s(\mu)}{\pi}\right)^3\sum_a\int dz\;D_a^\gamma(z,M_F)\;K^{\rm brems}_{\rm HO}[A+B\to a+X](p_{T\,\gamma},\mu,M)\,. \end{aligned} \tag{3.8}$$

In eq. (3.8), the M_F dependence of the HO corrections has been made explicit. The remainder of the HO corrections is given by $K^{\rm brems}_{\rm HO}$ and no longer depends on M_F. The kernels $P_{ia}(x)$ are the Altarelli-Parisi splitting functions.

The direct contribution has the following form:

$$\begin{aligned} d\sigma^{\rm dir}&[A+B\to\gamma+jet+x] = \\ &= 2\pi\left(\frac{\alpha_s(\mu)}{\pi}\right)\left(\frac{\alpha}{\pi}\right)\sum_b E_\gamma\frac{d\widehat{\sigma}_{\rm Born}[A+B\to\gamma+b]}{d\vec{p}_\gamma\;d\eta_b}d\eta_b\;d\eta_\gamma\;p_{T\,\gamma}\;dp_{T\,\gamma}\;+ \\ &\quad+\;2\pi\left(\frac{\alpha_s(\mu)}{\pi}\right)^2\left(\frac{\alpha}{\pi}\right)\sum_{\substack{a,b\\ a=q,\bar{q}}}\int_{z_{\min}}^1 dz\;e_a^2\;P_{\gamma q}(z)\;\ln\left(\frac{p_{T\,\gamma}}{M_F}\right)\times \\ &\qquad\times\;E_a\frac{d\widehat{\sigma}_{\rm Born}[A+B\to a+b]}{d\vec{p}_a\;d\eta_b}d\eta_b\;d\eta_a\;p_{T\,a}\;dp_{T\,a}\;+ \\ &\quad+\;2\pi\left(\frac{\alpha_s(\mu)}{\pi}\right)^2\left(\frac{\alpha}{\pi}\right)\;K^{\rm dir}_{\rm HO}[A+B\to\gamma+jet+X](p_{T\,\gamma},\mu,M)\,. \end{aligned} \tag{3.9}$$

Here we have included QCD corrections up to NLO and also made the M_F dependence of the HO corrections explicit. The splitting function $P_{\gamma q}(z)$ of a quark q into a photon is

$$P_{\gamma q}(z) = \frac{1+(1-z)^2}{z}\,. \tag{3.10}$$

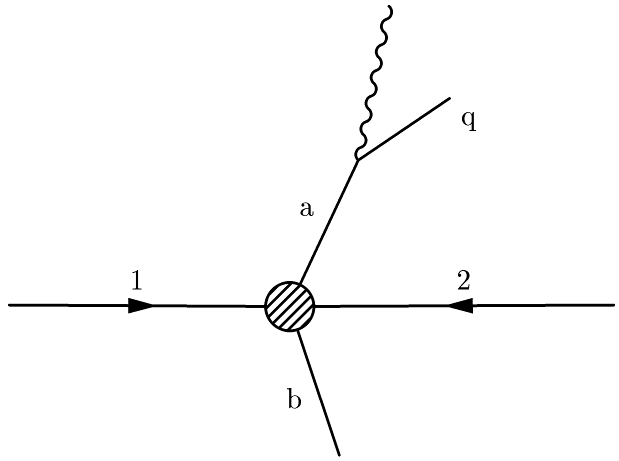

Figure 1: Kinematics of HO corrections to the direct contribution.

The LO evolution equations satisfied by the fragmentation functions are

$$M_F^2 \frac{\partial D_a^\gamma(z, M_F)}{\partial M_F^2} = \frac{\alpha}{2\pi} \, e_a^2 \; P_{\gamma q}(z) + \frac{\alpha_s}{2\pi} \left[\sum_q (P_{qa} + P_{\bar{q}a}) \otimes D_q^\gamma(M_F) + \right. \\ \left. + P_{ga} \otimes D_g^\gamma(M_F) \right], \tag{3.11}$$

where the symbol $\otimes$ denotes convolutions with respect to the momentum fraction z, and e_a is the electric charge of the parton a. Using eq. (3.11), it is straightforward to verify the M_F-independence of the prompt-photon cross section up to NLO accuracy.

A short description of the derivation of eq. (3.9) is instructive and helps to understand how the isolated cross section (see section 5) can be obtained from the inclusive cross section. Let us consider the subprocess $1 + 2 \to \gamma + q + b$, in which the photon is emitted by the final-state quark a (figure 1). Its contribution to the cross section is

$$d\sigma = \int dx_1 \; G_{1/A}(x_1) \; dx_2 \; G_{2/B}(x_2) \times \\ \times \frac{1}{2\hat{s}} |\overline{\mathcal{M}}|^2 \widetilde{dp}_\gamma \; \widetilde{dp}_q \; \widetilde{dp}_b \; (2\pi)^n \; \delta^{(n)} \left(p_1 + p_2 - p_b - p_\gamma - p_q \right), \tag{3.12}$$

where we use the definition $\widetilde{dp} \equiv d^n p \; \delta^{(+)}(p^2)/(2\pi)^{n-1}$, and $n = 4 - 2\varepsilon$ is the number of space-time dimensions. We are mainly interested in the singular contribution (non-collinear contributions are discussed in section 6) to eq. (3.12) coming from the configuration in which the final-state quark and the photon are collinear. Therefore the matrix element of the subprocess $1 + 2 \to \gamma + q + b$ can be approximated as

$$|\overline{\mathcal{M}}|^2 \simeq \frac{e_q^2 \mu^{2\varepsilon}}{p_\gamma \cdot p_q} \left(P_{\gamma q}(z) - \varepsilon z \right) |\overline{\mathcal{M}}_B|^2 \,, \tag{3.13}$$

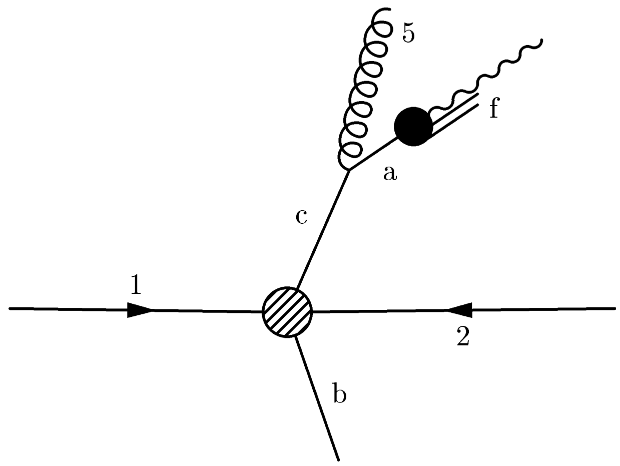

Figure 2: Kinematics of HO corrections to the fragmentation contribution.

where $\mathcal{M}_B$ is the Born-level amplitude of the subprocess $1+2 \to a+b$ in figure 1, and we defined the longitudinal variable z as follows:

$$z = \frac{p_{T\,\gamma}}{p_{T\,\gamma} + p_{T\,q}} \, . \tag{3.14}$$

Inserting eq. (3.13) in eq. (3.12), we obtain

$$\begin{aligned} d\sigma = \frac{V(n-2) e_q^2 \mu^{2\varepsilon}}{2^3 (2\pi)^{2n-3} S^2} \int \frac{dx_1}{x_1} \frac{dx_2}{x_2} \; G(x_1, M) \; G(x_2, M) \; (P_{\gamma q}(z) - \varepsilon z) \, |\overline{\mathcal{M}}_B|^2 \; p_{T\,\gamma}^{n-3} \times \\ \times \; dp_{T\,\gamma} \; d\eta_\gamma \; d\eta_b \delta \left(x_1 - \frac{\sum_i p_i^{(+)}}{\sqrt{S}} \right) \delta \left(x_2 - \frac{\sum_i p_i^{(-)}}{\sqrt{S}} \right) \frac{d^{n-2} p_q \; d\eta_q}{p_q \cdot p_\gamma} \, , \end{aligned} \tag{3.15}$$

where η_i are the pseudorapidities, $p_{T\,b} = |\vec{p}_{T\,q} + \vec{p}_{T\gamma}|$, and we have defined

$$\sum_i p_i^{(\pm)} = p_{T\,\gamma} e^{\pm \eta_\gamma} + p_{T\,q} e^{\pm \eta_q} + p_{T\,b} e^{\pm \eta_b} \, .$$

The factor $V(n-2) = 2\pi^{\frac{n-2}{2}} / \Gamma(\frac{n-2}{2})$ comes from the integration over the azimuthal angle of the photon. The phase space in eq. (3.15) can be written in terms of the variable z in eq. (3.14) and the difference ϕ_q between the azimuthal angles of the quark and the photon:

$$\begin{aligned} \mu^{2\varepsilon} \int \frac{d^{n-2} p_q \; d\eta_q}{p_q \cdot p_\gamma} &= V(n-3) \mu^{2\varepsilon} \int \frac{(\sin \phi_q)^{-2\varepsilon} \; d\phi_q \; d\eta_q}{\cosh(\eta_\gamma - \eta_q) - \cos \phi_q} \; \frac{p_{T\,q}^{n-3} \; dp_{T\,q}}{p_{T\,q} \; p_{T\,\gamma}} \\ &= V(n-3) \left(\frac{\mu^2}{p_{T\,\gamma}^2} \right)^{\varepsilon} \int \frac{(\sin \phi_q)^{-2\varepsilon} d\phi_q d\eta_q}{\cosh(\eta_\gamma - \eta_q) - \cos \phi_q} \left(\frac{1-z}{z} \right)^{n-4} \frac{dz}{z^2} \, . \end{aligned} \tag{3.16}$$

For the purpose of the discussion on isolated photons in section 5, we restrict the angular integration in eq. (3.16) to a cone of radius R in the η-ϕ space around the photon. This restriction does not change the singular collinear term (proportional to the pole $1/\varepsilon$) we are interested in. On the other hand, this produces a dependence on $\ln R^2$ that we are going to use in section 5. In the small-cone approximation defined by the constraint

$\Theta(R^2 - \phi_q^2 - (\eta_\gamma - \eta_q)^2)$ with $R^2 \ll 1$, we can obtain a simple expression for the cross section. Using collinear expressions for the kinematic variables and defining the quark momentum $p_a = p_\gamma + p_q$, we have

$$\begin{aligned} p_{T\,a} &\simeq \frac{p_{T\,\gamma}}{z}, \qquad p_{T\,b} \simeq p_{T\,a}, \\ \eta_q &= \eta_\gamma, \qquad \sum_i p_i^{(\pm)} \simeq \frac{p_{T\,\gamma}}{z}\left(e^{\pm\eta_\gamma} + e^{\pm\eta_b}\right). \end{aligned} \tag{3.17}$$

The integrations over η_q and ϕ_q in (3.16) are easily performed, and we finally obtain (neglecting terms of $\mathcal{O}\left(R^2\right)$)

$$\begin{aligned} d\sigma^{\rm cone} &= \frac{V(n-2)p_{T\,\gamma}^{n-3}}{2^2(2\pi)^{n-2}S^2}\int \frac{G_{1/A}(\widehat{x}_1, M)}{\widehat{x}_1}\,\frac{G_{2/B}(\widehat{x}_2, M)}{\widehat{x}_2}\,|\overline{\mathcal{M}}_B|^2 p_{T\,a}^{n-3}\, dp_{T\,a}\, d\eta_a\, d\eta_b \times \\ &\quad \times \frac{\alpha}{2\pi}e_a^2\left(P_{\gamma q}(z) - \varepsilon z\right)\left(-\frac{1}{\varepsilon}\right)\frac{\Gamma(1-\varepsilon)}{\Gamma(1-2\varepsilon)}\left(\frac{4\pi\mu^2}{R^2 p_{T\,\gamma}^2(1-z)^2}\right)^{\varepsilon} dz\,, \end{aligned} \tag{3.18}$$

where the variables $\widehat{x}_i$ are given by

$$\widehat{x}_{\substack{1\\2}} = \frac{p_{T\,\gamma}}{z\sqrt{S}}\left(e^{\pm\eta_\gamma} + e^{\pm\eta_b}\right).$$

Equation (3.18) can be rewritten as

$$\begin{aligned} d\sigma^{\rm cone} &= 2\pi\left(\frac{\alpha_s(\mu)}{\pi}\right)^2 \int_{z_{\rm min}}^1 E_a\frac{d\widehat{\sigma}_{\rm Born}(A+B\to a+b)}{d\vec{p}_a\, d\eta_b}\, d\eta_b\, d\eta_a\, p_{T\,a}^{n-3}\, dp_{T\,a} \times \\ &\quad \times \left\{D_a^\gamma(z, M_F) + \frac{\alpha}{2\pi}e_a^2\left[2\ln\left(\frac{R\, p_{T\,\gamma}\,(1-z)}{M_F}\right)P_{\gamma q}(z) + z\right]\right\} dz\,, \end{aligned} \tag{3.19}$$

where we have used the lowest-order definition of the quark into a photon fragmentation function in the $\overline{MS}$ factorization scheme:

$$D_q^\gamma(z, M_F, \varepsilon) \equiv -\frac{1}{\varepsilon}\frac{\Gamma(1-\varepsilon)}{\Gamma(1-2\varepsilon)}\left(\frac{4\pi\mu^2}{M_F^2}\right)^{\varepsilon}\frac{\alpha}{2\pi}e_q^2 P_{\gamma q}(z)\,. \tag{3.20}$$

We clearly recognize two parts in eq. (3.19). The part proportional to $D_q^\gamma(z, M_F)$, which comes from the collinear pole $1/\varepsilon$ in eq. (3.18), is nothing but the Born-level fragmentation component in (3.4). The remaining part contributes to the direct component in eq. (3.9). Since it has been calculated in the collinear approximation, it only contains terms that are either proportional to $\ln R$ or constant in the limit $R \to 0$. Among the constant terms there is the term proportional to $\ln(p_{T\,\gamma}/M_F)$, which was explicitly written in (3.9).

The contribution to the direct component of the inclusive cross section coming from the region outside the cone cannot be evaluated so straightforwardly, yet it must contain a term proportional to $\ln(1/R)$ of the form

$$\begin{aligned} d\sigma^{\rm outside} &= 2\pi\left(\frac{\alpha_s(\mu)}{\pi}\right)^2 \int_{z_{\rm min}}^1 E_a\frac{d\widehat{\sigma}_{\rm Born}(A+B\to a+b)}{d\vec{p}_a\, d\eta_b} \\ &\quad \times d\eta_b\, d\eta_a\, p_{T\,a}^{n-3}\, dp_{T\,a}\frac{\alpha}{2\pi}e_a^2\left[2\ln\left(\frac{1}{R}\right)P_{\gamma q}(z)\right] dz\,. \end{aligned} \tag{3.21}$$

Indeed, the R dependence must cancel in the sum of the contributions from inside and from outside the cone.

The NLO calculation described so far is extended to the case of isolated photons in section 5. Before doing that, we discuss the validity of factorization of isolated photons at any order in QCD perturbation theory.

4. Isolated-particle production and factorization

When no isolation criterion is applied, the inclusive photon cross section is computable by using the QCD factorization formula (3.1). The formula states that at large values of $p_{T\,\gamma}$ the short-distance dynamics is perturbatively computable in terms of partonic cross sections, while the dominant non-perturbative phenomena can be factorized in the parton densities of the colliding hadrons and the fragmentation function of the detected photon. Owing to the inclusiveness of the process, all the remaining non-perturbative effects have the form $(Q_0/p_{T\,\gamma})^p$ and are suppressed by some inverse power p of the photon transverse momentum. These terms are not indicated on the right-hand side of eq. (3.1), since they are negligible as long as $p_{T\,\gamma}$ is much larger than the typical hadronic scale $Q_0 \sim \mathcal{O}(1\,\mathrm{GeV})$.

In the case of isolated photons, the isolation criterion (1.1) enforces additional phase-space restrictions. This implies that the cross section is *no* longer fully inclusive over the hadronic final state and, hence, that the factorized expression (3.1) is not necessarily valid [10, 19, 20, 21]. This issue was considered in ref. [21], where factorization was proved at *any* order in QCD perturbation theory in the case of the isolation criterion of eq. (3.1). The discussion in ref. [21] was mainly focused on prompt-photon production in e^+e^- collisions. To better clarify the differences between e^+e^- collisions and hadron-hadron collisions, in the following we reconsider in more detail the latter case.

In the theoretical literature (see e.g. refs. [10, 11]) on isolated-photon production at hadron colliders, the isolation criterion (1.1) is sometime replaced by a similar one, in which the isolation is defined by an upper limit $E_{\rm max}$ on the accompanying *hadronic energy* $E^{\rm had}$ in the c.m. frame rather than by an upper limit $E_{T\,\rm max}$ on the hadronic transverse energy $E_T^{\rm had}$. To discuss both criteria in a unified manner, we introduce a more exclusive definition of the isolation. The photon is isolated if the total hadronic four-momentum $Q_\mu^{\rm had}$ inside the isolation cone is *fixed* at a given value Q_μ:

$$Q_\mu^{\rm had} = Q_\mu\,, \qquad \text{inside } (y-y_\gamma)^2 + (\phi-\phi_\gamma)^2 \le R^2\,. \tag{4.1}$$

The cross section corresponding to this generalized isolation is denoted by $d\sigma^{g-{\rm is}}/d^4Q$. From it, we can recover the cross section $\sigma^{\rm is}$ corresponding to the criterion in eq. (1.1) by simply integrating over Q_μ as

$$\sigma^{\rm is} = \int d^4Q\, \frac{d\sigma^{g-{\rm is}}}{d^4Q}\, \Theta(E_{T\,\rm max} - E_T)\,, \tag{4.2}$$

where E_T denotes the transverse energy of the four-momentum Q_μ. We can also replace the hadronic transverse energy with the hadronic energy in the isolation criterion (1.1), by simply replacing the transverse energies $E_{T\,\rm max}, E_T$ with the corresponding c.m. energies $E_{\rm max}, E$ in the argument of the Θ-function on the right-hand side of eq. (4.2). In the following we discuss factorization for the generalized isolated cross section $d\sigma^{g-{\rm is}}/d^4Q$.

JHEP05(2002)028

Our proof of factorization is based on the consistency, at the level of *power unsuppressed* contributions, between QCD perturbation theory and the full QCD theory. We exploit the formal correspondence between singularities in the calculation at the parton level and non-perturbative effects. Since the hadronic cross section is computable and finite in the full theory, the presence of singularities that are not cancelled or not factorizable at the parton level implies that of compensating singularities of non-perturbative origin. Thus, we are led to consider the perturbative singular behaviour, which is due to the emission of soft and collinear partons. This picture obviously agrees with the physical expectation that factorization can only be spoiled by long-distance phenomena, such as those involving soft and collinear radiation.

To give our formal proof, we consider the production of the prompt photon with momentum p_γ in the collisions of two hadrons H_A and H_B with momenta p_A and p_B. In general, the hadronic final state contains $n+1$ (with $n \geq 0$, since the transverse momentum of the photon has to be balanced by some final-state radiation) additional partons (hadrons) with momenta $p_1, \dots, p_{n+1}$. Any isolation criterion applied to the photon is thus specified in terms of a function

$$F_{\{\rm is\}}^{(n+1)}(p_A, p_B; p_\gamma; p_1, \dots, p_{n+1}) \tag{4.3}$$

that depends on the momenta of the particles in the event. The subscript $\{\rm is\}$ denotes the dependence on the isolation parameters, whose precise definition is not explicitly spelled out for the moment. The factorization of the prompt-photon cross section with isolation can be studied [31, 32, 33] in terms of the properties of the isolation function in eq. (4.3). More precisely, factorization is valid provided $F_{\{\rm is\}}$ fulfils the following requirements[2]

i) infrared safety:

$$F_{\{\rm is\}}^{(n\boldsymbol{+1})}(p_A, p_B; p_\gamma; p_1, \dots, \boldsymbol{p}_i, \dots, p_{n+1}) \underset{p_i \to 0}{\longrightarrow} F_{\{\rm is\}}^{(n)}(p_A, p_B; p_\gamma; p_1, \dots, p_{n+1}) \, , \tag{4.4}$$

ii) collinear safety:

$$\begin{aligned} F_{\{\rm is\}}^{(n\boldsymbol{+1})}(p_A, p_B; p_\gamma; p_1, \dots, \boldsymbol{p}_i, \boldsymbol{p}_j, \dots, p_{n+1}) &\underset{p_i \parallel p_j}{\longrightarrow} \\ \underset{p_i \parallel p_j}{\longrightarrow} F_{\{\rm is\}}^{(n)}(p_A, p_B; p_\gamma; p_1, \dots, \boldsymbol{p_i} + \boldsymbol{p_j}, \dots, p_{n+1}) \, , \end{aligned} \tag{4.5}$$

iii) final-state collinear factorizability:

$$\begin{aligned} F_{\{\rm is\}}^{(n\boldsymbol{+1})}(p_A, p_B; \boldsymbol{p}_\gamma; p_1, \dots, \boldsymbol{p}_i, \dots, p_{n+1}) &\underset{p_i \parallel p_\gamma}{\longrightarrow} \\ \underset{p_i \parallel p_\gamma}{\longrightarrow} F_{\{\rm is\}}^{(n)}(p_A, p_B; \boldsymbol{p_\gamma} + \boldsymbol{p_i}; p_1, \dots, \dots, p_{n+1}) \, , \end{aligned} \tag{4.6}$$

iv) initial-state collinear factorizability:

$$\begin{aligned} F_{\{\rm is\}}^{(n\boldsymbol{+1})}(\boldsymbol{p}_A, p_B; p_\gamma; p_1, \dots, \boldsymbol{p}_i, \dots, p_{n+1}) &\underset{p_i \parallel p_A}{\longrightarrow} \\ \underset{p_i \parallel p_A}{\longrightarrow} F_{\{\rm is\}}^{(n)}(\boldsymbol{p_A} - \boldsymbol{p_i}, p_B; p_\gamma; p_1, \dots, \dots, p_{n+1}) \, . \end{aligned} \tag{4.7}$$

Of course, the analogue of eq. (4.7) with $p_A \leftrightarrow p_B$ is understood.

[2]In eqs. (4.4)–(4.7) bold-face characters are used just to emphasize the differences between left-hand and right-hand sides.

The requirement of i) infrared safety means that the cross section is insensitive to the momenta of arbitrarily soft particles. The requirement of ii) collinear safety implies that, when some final-state particles are produced collinearly, the cross section depends on their total momentum rather than on the momentum of each of them. The general isolation criterion in eq. (4.1) depends on $Q_\mu = Q_\mu^{\rm had} = \sum_{j\in {\rm cone}} p_{\mu\, j}$, the total hadronic momentum inside the isolation cone. Since $Q_\mu^{\rm had}$ is an infrared- and collinear-safe quantity, the isolation criterion in eq. (4.1) fulfils eqs. (4.4) and (4.5).

The property in eq. (4.6) guarantees that all the long-distance phenomena related to the low-momentum fragmentation of the photon can be absorbed and factorized in the universal fragmentation function $D_a^\gamma(z; M_F)$. By universal we mean that it does not depend on the process and, in particular, it does not depend on the isolation parameters. Naive inspection of the isolation criterion in eq. (4.1) may suggest that it violates eq. (4.6). As pointed out in ref. [21], this is not the case.

To explain the key point [21], let us first consider the following isolation criterion:

$$F^{(n+1)}_{\{Q^{\rm cut},R\}}(p_A,p_B;p_\gamma;p_1,\dots,p_{n+1}) = \delta^{(4)}\left(Q^{\rm cut} - \left[p_\gamma + \sum_{j=1}^{n+1} p_j \; \Theta(R-R_{j\gamma}) \right] \right) , \tag{4.8}$$

where

$$R_{j\gamma} = \sqrt{(y_j-y_\gamma)^2 + (\phi_j-\phi_\gamma)^2}\,, \tag{4.9}$$

and R and $Q_\mu^{\rm cut}$ are *external* isolation parameters. The term in the square bracket on the right-hand side of eq. (4.8) is the total (hadron+photon) four-momentum inside the cone of radius R. Thus we have

$$p_\gamma + \sum_{j=1}^{n+1} p_j \; \Theta(R-R_{j\gamma}) \;\underset{p_i \,\parallel\, p_\gamma}{\longrightarrow}\; (p_\gamma+p_i) + \sum_{\substack{j=1\\ j\neq i}}^{n+1} p_j \; \Theta(R-R_{j\gamma})\,, \tag{4.10}$$

and the function $F^{(n+1)}_{\{Q^{\rm cut},R\}}$ fulfils eq. (4.6).

Then, we can observe that the momentum p_γ of the photon and the isolation parameter Q_μ in eq. (4.1) are both kept fixed in the measurement of the cross section, so they can be regarded as *external* variables that are independent of the momenta $p_A, p_B, p_\gamma, p_1, \dots, p_{n+1}$. Therefore, by simply making the identification

$$Q_\mu^{\rm cut} = Q_\mu + p_{\mu\,\gamma}\,, \tag{4.11}$$

the isolation criterion in eq. (4.1) can be recast in the form of eq. (4.8), which manifestly satisfies eq. (4.6).

The properties in eqs. (4.4)–(4.6) are sufficient to prove factorization in the case of e^+e^- collisions [21]. In hadron-hadron collisions, the cross section is affected by additional long-distance phenomena related to the non-perturbative binding of the colliding partons into the incoming hadrons. At the parton level, these phenomena lead to initial-state collinear singularities that have to be absorbed and factorized in the non-perturbative parton distributions of the hadrons H_A and H_B. The property in eq. (4.7) guarantees that the photon-isolation criterion does not spoil the factorization of the initial-state collinear singularities.

Since the expression on the right-hand side of eq. (4.8) does not explicitly depend either on the incoming momenta p_A, p_B or on any final-state momentum parallel to them, the property in eq. (4.7) is thus evidently fulfilled by the generalized isolation criterion in eq. (4.1).

The main conclusion of our discussion on the generalized isolation criterion in eq. (4.1) is that QCD factorization is valid at *any* order in perturbation theory. Factorization for the isolation criterion (1.1) with respect to the hadronic transverse energy (or to the hadronic energy) thus follows from eq. (4.2). Note, however, that $d\sigma^{g-\mathrm{is}}/d^4Q$ factorizes as a function of the fixed isolation parameter Q_μ^{cut} rather than as a function of Q_μ (see eqs. (4.8) and (4.11)). As discussed below, this functional dependence has influence upon the kinematical structure of the factorization formula for the isolated cross sections.

We first discuss the isolation criterion (1.1) with respect to the hadronic transverse energy. Since $d\sigma^{g-\mathrm{is}}/d^4Q$ factorizes at fixed $Q_\mu^{\mathrm{cut}} = Q_\mu + p_{\mu\,\gamma}$, the constrained integration in eq. (4.2) leads to a dependence on the variable E_T^{cut}:

$$E_T^{\mathrm{cut}} = E_{T\ \max} + E_{T\,\gamma} = E_{T\ \max} + p_{T\,\gamma}\,. \tag{4.12}$$

The inclusive cross section is thus a function on the photon momentum p_γ and on the isolation parameters R and E_T^{cut}. It is convenient to define the variable

$$z_c \equiv \frac{p_{T\,\gamma}}{E_T^{\mathrm{cut}}} = \frac{p_{T\,\gamma}}{E_{T\ \max} + p_{T\,\gamma}} < 1\,. \tag{4.13}$$

The inclusive distribution $d\sigma^{\mathrm{is}}/dp_{T\,\gamma}dy_\gamma$ with transverse-energy isolation, which we simply denote by $\sigma^{\mathrm{is}}(p_\gamma; z_c, R)$, fulfils a factorization formula analogous to eq. (3.1):

$$\begin{aligned}
\sigma^{\mathrm{is}}(p_\gamma; z_c, R) &= \sum_a \int_0^1 \frac{dz}{z}\, \widehat{\sigma}^{a,\mathrm{is}}\left(\frac{p_\gamma}{z}; \frac{z_c}{z}, R; \mu, M, M_F\right) D_a^\gamma(z; M_F) + \\
&\quad + \widehat{\sigma}^{\gamma,\mathrm{is}}(p_\gamma; z_c, R; \mu, M, M_F) \\
&= \sum_a \int_0^1 \frac{dz}{z}\, \widehat{\sigma}^{a,\mathrm{is}}\left(\frac{p_\gamma}{z}; \frac{z_c}{z}, R; \mu, M, M_F\right) D_a^\gamma(z; M_F)\, \Theta(z - z_c) + \\
&\quad + \widehat{\sigma}^{\gamma,\mathrm{is}}(p_\gamma; z_c, R; \mu, M, M_F)\,.
\end{aligned} \tag{4.14}$$

The fragmentation function $D_a^\gamma(z; M_F)$ is the same fragmentation function as appears in the non-isolated case. In particular, it does not depend on the isolation parameters. The dependence on the latter is fully embodied in the subprocess cross sections $\widehat{\sigma}^{a,\mathrm{is}}$ and $\widehat{\sigma}^{\gamma,\mathrm{is}}$, which, respectively, give the fragmentation and direct contributions to the hadronic cross section. We recall that the subprocess cross sections $\widehat{\sigma}^{a,\mathrm{is}}$ and $\widehat{\sigma}^{\gamma,\mathrm{is}}$ are obtained by convoluting the parton densities of the colliding hadrons with the cross sections $\widehat{\sigma}_{ij}^{a,\mathrm{is}}$ and $\widehat{\sigma}_{ij}^{\gamma,\mathrm{is}}$ of the partonic subprocesses $i + j \to a + X$ and $i + j \to \gamma + X$. We have

$$\begin{aligned}
\widehat{\sigma}^{a,\mathrm{is}}\left(\frac{p_\gamma}{z}; \frac{z_c}{z}, R; \mu, M, M_F\right) &= \sum_{i,j} \int_0^1 dx_1\, dx_2\, G_{i/A}(x_1, M)\, G_{j/B}(x_2, M) \times \\
&\quad \times \widehat{\sigma}_{ij}^{a,\mathrm{is}}\left(x_1 p_A, x_2 p_B, \frac{p_\gamma}{z}; \frac{z_c}{z}, R; \mu, M, M_F\right),
\end{aligned} \tag{4.15}$$

and a similar formula relates $\widehat{\sigma}^{\gamma,\mathrm{is}}$ to $\widehat{\sigma}_{ij}^{\gamma,\mathrm{is}}$.

Note that, according to eqs. (4.8) and (4.2), factorization holds at fixed $E_T^{\rm cut}$. Since z_c is obtained by rescaling $E_T^{\rm cut}$ with the factor $p_{T\,\gamma}$, the variable z_c is a *scaling* variable with respect to factorization. In other words, the partonic cross section in eq. (4.14) depends on p_γ/z and z_c/z. In particular, since z_c is constrained to be $z_c < 1$ from eqs. (4.8) and (4.2), this constraint propagates to $\widehat{\sigma}^{a,{\rm is}}(p_\gamma/z; z_c/z)$ as $z_c/z < 1$. We made this condition explicit in eq. (4.14).

In current experimental practice, $E_{T\,\max}$ is sometimes expressed in terms of the dimensionless parameter ε_h defined by

$$\varepsilon_h = \frac{E_{T\,\max}}{p_{T\,\gamma}}\,. \tag{4.16}$$

This parameter is related to our scaling variable z_c by

$$z_c = \frac{1}{1+\varepsilon_h}\,. \tag{4.17}$$

The partonic cross sections in eq. (4.14) can be expanded as power series in α_s analogously to the fully inclusive case in eqs. (4.18) and (3.3). Actually, at the Born level, it is straightforward to show [10] that $\widehat{\sigma}^{\gamma,{\rm is}}$ and $\widehat{\sigma}^{a,{\rm is}}$ exactly coincide with the corresponding expression for the non-isolated case, apart from the overall constraint $z_c/z < 1$ mentioned above. Up to NLO, we thus have

$$\begin{aligned}\widehat{\sigma}^{\gamma,{\rm is}}(p; z_c, R; \mu, M, M_F) &= \left(\frac{\alpha_s(\mu)}{\pi}\right)\,\sigma^{\gamma}_{\rm Born}(p; M) + \\ &\quad + \left(\frac{\alpha_s(\mu)}{\pi}\right)^2 \sigma^{\gamma,{\rm is}}_{\rm HO}(p; z_c, R; \mu, M, M_F)\,, \end{aligned}\tag{4.18}$$

$$\begin{aligned}\widehat{\sigma}^{a,{\rm is}}(p; z_c, R; \mu, M, M_F) &= \left(\frac{\alpha_s(\mu)}{\pi}\right)^2 \sigma^{a}_{\rm Born}(p; M) + \\ &\quad + \left(\frac{\alpha_s(\mu)}{\pi}\right)^3 \sigma^{a,{\rm is}}_{\rm HO}(p; z_c, R; \mu, M, M_F)\,. \end{aligned}\tag{4.19}$$

In the following sections we compute the NLO terms $\sigma^{\gamma,{\rm is}}_{\rm HO}$ and $\sigma^{a,{\rm is}}_{\rm HO}$.

We can now consider the variant of the isolation criterion (1.1) with respect to the hadronic c.m. energy. We can straightforwardly follow the previous discussion on transverse-energy isolation. The transverse-energy isolation parameter $E_T^{\rm cut}$ in eq. (4.12) and the scaling variable z_c in eq. (4.13) have to be, respectively, replaced by the energy isolation parameter $E^{\rm cut}$ and the scaling variable z_c^E:

$$E^{\rm cut} = E_{\max} + E_\gamma\,, \qquad z_c^E \equiv \frac{E_\gamma}{E^{\rm cut}} = \frac{E_\gamma}{E_{\max}+E_\gamma} < 1\,. \tag{4.20}$$

Denoting by $\sigma^{E-{\rm is}}$ the energy-isolation variant of the inclusive distribution $\sigma^{\rm is}$, we still have a factorization formula analogous to eq. (4.14): it is sufficient to make the formal replacements

$$\begin{aligned}\sigma^{\rm is}(p_\gamma; z_c, R) &\longrightarrow \sigma^{E-{\rm is}}(p_\gamma; z_c^E, R)\,, \\ \widehat{\sigma}^{\rm is}\left(\frac{p_\gamma}{z}; \frac{z_c}{z}, R; \mu, M, M_F\right) &\longrightarrow \widehat{\sigma}^{E-{\rm is}}\left(\frac{p_\gamma}{z}; \frac{z_c^E}{z}, R; \mu, M, M_F\right), \qquad z_c \longrightarrow z_c^E\,. \end{aligned}\tag{4.21}$$

In particular, the fragmentation function $D_a^\gamma(z;M_F)$ is not affected by the change of the isolation criterion. Note, however, that the strict formal correspondence between the two variants of the isolation criterion does not extend to the cross sections of the partonic subprocesses $i+j \to a+X$ and $i+j \to \gamma+X$. In fact, although the convolution structure of eq. (4.15) is still valid, we have to perform the following replacement:

$$\begin{aligned}
&\widehat{\sigma}_{ij}^{a,\mathrm{is}}\left(x_1p_A, x_2p_B, \frac{p_\gamma}{z}; \frac{z_c}{z}, R; \mu, M, M_F\right) \longrightarrow \\
&\qquad \longrightarrow \widehat{\sigma}_{ij}^{a,E-\mathrm{is}}\left(x_1p_A, x_2p_B, \frac{p_\gamma}{z}; \frac{z_c^E}{z}, R, \frac{E^{\mathrm{cut}}}{x_1\sqrt{S}}, \frac{E^{\mathrm{cut}}}{x_2\sqrt{S}}; \mu, M, M_F\right). \qquad (4.22)
\end{aligned}$$

Unlike $\widehat{\sigma}_{ij}^{a,\mathrm{is}}$, its energy-isolation variant $\widehat{\sigma}_{ij}^{a,E-\mathrm{is}}$ does depend on $E^{\mathrm{cut}}/x_1\sqrt{S}$ and $E^{\mathrm{cut}}/x_2\sqrt{S}$. This additional dependence follows from having defined isolation with respect to the hadronic energy in the c.m. frame. Such a definition is not invariant under longitudinal boosts along the beam direction, thus leading to an entangled dependence on E^{cut} and on the energies $x_1\sqrt{S}/2, x_2\sqrt{S}/2$ of the partonic beams. In other words, the dependence on the isolation parameter E^{cut} is not *kinematically* factorized [21] from the dependence on the momentum fractions in the parton densities.

Despite the formal correspondence in eq. (4.21), beyond the LO, the functional dependence of $\sigma^{E-\mathrm{is}}$ on z_c^E and R is not the same as the functional dependence of σ^{is} on z_c and R. However, the transverse-energy fraction $\sum_j E_{T\,j}/E_{T\,\gamma}$ and the c.m.-energy fraction $\sum_j E_j/E_\gamma$ coincide as long as all the partons (hadrons) j inside the isolation cone are either soft or collinear to the photon direction. This implies that the two variants of the isolation criterion can *substantially* differ only if the isolation cone contains at least one *hard* parton that is not collinear to the photon. Such a kinematical configuration is suppressed both in the (soft) limit $z_c \to 1$ and in the (collinear) limit $R \to 0$. In either of these limits, the two variants of the isolation criterion perturbatively coincide: the order-by-order perturbative calculations of σ^{is} and $\sigma^{E-\mathrm{is}}$ differ by terms that are of $\mathcal{O}(1-z_c)$, when $z_c \to 1$, and of $\mathcal{O}(R^2)$, when $R \to 0$.

The validity of factorization implies that the partonic cross sections in eqs. (4.18) and (4.19) are computable in QCD perturbation theory. Nonetheless, their fixed-order perturbative expansions are not always well behaved. This is the case, for instance, in the kinematical configurations of highly isolated photons $(1-z_c \ll 1)$ and of very small isolation cones $(R \ll 1)$. When $1-z_c \ll 1$, the fixed-order expansion contains large double-logarithmic contributions, $(\alpha_s \ln^2(1-z_c))^n$, of soft origin. When $R \ll 1$, the fixed-order expansion contains large single-logarithmic contributions, $(\alpha_s \ln R)^n$, of collinear origin. The effects of these logarithmic contributions at NLO are discussed in section 6.

Another general source of misbehaviour in the fixed-order expansion of perturbatively computable observables is the possible presence of integrable logarithmic singularities at some "critical" points away from the soft and collinear boundaries of the phase space [34]. Such singularities occur [19, 20, 21] in the spectrum of isolated prompt photons produced in e^+e^- collisions, and are located at the critical point $2E_\gamma = z_c^E\sqrt{S}$ (in e^+e^- collisions, the isolation is defined with respect to the c.m. energies). The partonic cross section $\sigma_{ij}^{a,\mathrm{is}}$ (or $\sigma_{ij}^{a,E-\mathrm{is}}$) in eq. (4.22) has an analogous critical point at $2E_{T\,\gamma} = z_c\sqrt{x_1x_2S}/\cosh y_\gamma^*$ (or

$2E_{T\,\gamma} = z_c^E \sqrt{x_1 x_2 S}/\cosh y_\gamma^*)$, where $y_\gamma^* = y_\gamma - \ln\sqrt{x_1/x_2}$ is the photon rapidity in the partonic c.m. frame. Unlike the c.m. energy $\sqrt{S}$ in e^+e^- collisions, the partonic c.m. energy $\sqrt{\hat{s}} = \sqrt{x_1 x_2 S}$ is not fixed and depends on the momentum fractions x_1 and x_2 of the colliding partons. Any possible *integrable* singularities in the partonic cross sections $\sigma_{ij}^{a,\mathrm{is}}$ thus disappear after integration over x_1 and x_2 (see eq. (4.15)). In conclusion, there are no critical points in the single-photon inclusive cross sections $\sigma^{\mathrm{is}}(p_\gamma; z_c, R)$, $\widehat{\sigma}^{\gamma,\mathrm{is}}(p; z_c, R; \mu, M, M_F)$ and $\widehat{\sigma}^{a,\mathrm{is}}(p; z_c, R; \mu, M, M_F)$ (see eqs. (4.14), (4.18) and (4.19)) in which we are interested throughout the present paper. Note, however, that critical points and related integrable singularities occur in less inclusive distributions of isolated prompt photons produced in hadron-hadron collisions (see e.g. ref. [35]).

The photon isolation procedure actually implemented by the D0 Collaboration [4] does not exactly coincide with the isolation criterion in eq. (1.1). A cone of radius R around the photon direction is still considered, but the upper limit $E_{T\,\max}$ is enforced on the hadronic transverse energy inside an annular region of width ΔR ($\Delta R < R$), rather than on the hadronic transverse energy inside the whole cone. More precisely, eq. (1.1) is replaced by the following:

$$E_T^{\mathrm{had}}(R) - E_T^{\mathrm{had}}(R - \Delta R) \leq E_{T\,\max}\,, \tag{4.23}$$

where $E_T^{\mathrm{had}}(R)$ and $E_T^{\mathrm{had}}(R - \Delta R)$ are the hadronic transverse energies in the two cones of radius R and $R - \Delta R$, respectively. This criterion is thus specified by the isolation function

$$\begin{aligned} &F^{(n+1)}_{\{E_{T\,\max}, R, \Delta R\}}(p_A, p_B; p_\gamma; p_1, \ldots, p_{n+1}) = \\ &\quad = \Theta\left(E_{T\,\max} - \sum_{j=1}^{n+1} E_{T\,j}\; \Theta(R - R_{j\gamma})\; \Theta(R_{j\gamma} - R + \Delta R) \right). \end{aligned} \tag{4.24}$$

It is straightforward to check that the properties in eqs. (4.4)–(4.7) are fulfilled by eq. (4.24), so the criterion (4.23) fulfils factorization. However, the kinematical structure of the corresponding factorized cross section, denoted by $\sigma^{\mathrm{D0-is}}(p_\gamma; E_{T\,\max}, R, \Delta R)$, is different from that in eq. (4.14). We have:

$$\begin{aligned} &\sigma^{\mathrm{D0-is}}(p_\gamma; E_{T\,\max}, R, \Delta R) = \\ &\quad = \sum_a \int_0^1 \frac{dz}{z}\, \widehat{\sigma}^{a,\mathrm{D0-is}}\left(\frac{p_\gamma}{z}; E_{T\,\max}, R, \Delta R; \mu, M, M_F\right) D_a^\gamma(z; M_F) + \\ &\qquad + \widehat{\sigma}^{\gamma,\mathrm{D0-is}}(p_\gamma; E_{T\,\max}, R, \Delta R; \mu, M, M_F)\,. \end{aligned} \tag{4.25}$$

The differences between eqs. (4.14) and (4.25) arise from the fact that the criterion (4.23) does not constrain the hadronic transverse energy collinear to the photon. Thus the isolation parameter $E_{T\,\max}$ is not rescaled by the photon momentum fraction z when going from the hadronic cross section $\sigma^{\mathrm{D0-is}}$ on the left-hand side of eq. (4.25) to the partonic cross section $\widehat{\sigma}^{a,\mathrm{D0-is}}$ on the right-hand side. Correspondingly, the isolation procedure does not set any absolute lower limit (such as $z > z_c$ in eq. (4.14)) on the momentum fraction z in the photon fragmentation function. In particular, at the LO the isolated cross section

$\sigma^{\mathrm{D0-is}}$ exactly coincides with the non-isolated cross section in eq. (3.1). Of course, higher-order contributions to the isolated cross section are different from those to the non-isolated one, and tend to suppress the direct and fragmentation components.

We conclude this section with two general observations. We have explicitly discussed isolated-photon production only in the case of hadron-hadron collisions. However, our discussion straightforwardly applies also to photon-hadron and photon-photon collisions: it is sufficient to substitute the parton densities of the colliding hadron for those of the colliding photon. Analogously, the final-state isolated photon can be replaced by any final-state isolated hadron (e.g. a pion) by substituting the fragmentation functions of the photon for those of the hadron.

5. Isolated cross section

After the all-order proof of factorization, we explicitly study how the isolation criterion (1.1) modifies the inclusive cross section calculated at NLO. In particular, we show how the partonic cross sections $\sigma_{\mathrm{HO}}^{\gamma,\mathrm{is}}$ and $\sigma_{\mathrm{HO}}^{a,\mathrm{is}}$ depend on the cone size R. We also show how the constraint on the transverse energy inside the isolation cone can be translated into conditions on the integration range of the longitudinal variables in eqs. (3.8), (3.9) and (3.14). In our calculation we follow a procedure similar to that in refs. [9, 11]: we start from the inclusive cross section and "subtract" the contributions that do not fulfil the isolation criterion.

5.1 Direct contribution with isolation

Considering the $\mathcal{O}(\alpha\alpha_s^2)$ contribution to the direct component (see figure 1), when the momentum $\vec{p}_q$ of the final-state quark is inside the cone around the photon, the isolation criterion (1.1) can be written as

$$p_{T\,q} \le \varepsilon_h \; p_{T\,\gamma}\,,$$

or, equivalently,

$$\frac{p_{T\,\gamma}}{p_{T\,q}+p_{T\,\gamma}} \ge \frac{1}{1+\varepsilon_h} \equiv z_c\,. \tag{5.1}$$

Therefore, the contribution to the isolated cross section is obtained from that to the inclusive cross section by subtracting from the latter the part that violates the constraint (5.1).

In terms of the result in eq. (3.19), obtained within the collinear approximation, eq. (5.1) is implemented by the condition $z > z_c$. Therefore the direct contribution to the isolated cross section is obtained from eq. (3.19) by simply subtracting the term

$$\begin{aligned} d\sigma_{\gamma jet}^{\mathrm{direct,sub}} = 2\pi \left(\frac{\alpha_s(\mu)}{\pi}\right)^2 \sum_{\substack{b\\ a=q,\bar{q}}} \int_{z_{\min}}^{z_c} E_a \frac{d\widehat{\sigma}^{\mathrm{Born}}(A+B\to a+b)}{d\vec{p}_a\; d\eta_b}\, d\eta_b\, d\eta_a\, p_{T\,a}^{n-3}\, dp_{T\,a} \times \\ \times \frac{\alpha}{2\pi}\, e_a^2 \left[2\ln\left(\frac{R\, p_{T\,\gamma}\,(1-z)}{M_F}\right)\frac{1+(1-z)^2}{z}+z\right] dz\,. \end{aligned} \tag{5.2}$$

We recall that expression (5.2) has been obtained in the approximation $R \ll 1$. All the terms of $\mathcal{O}(R^{2n})$ $(n \ge 1)$ have been neglected and will be calculated as discussed in section 6.

Note that the particular choice $M_F = R\ p_{T\gamma}$ eliminates the R-dependence from eq. (5.2). The price to pay is the introduction of an additional R-dependence in other terms of the cross section, notably through the M_F-dependence of the fragmentation function.

Note also that when the momentum p_q of the final-state quark in figure 1 is outside the isolation cone, the isolation criterion (1.1) does not enforce any additional constraint. In particular, the HO contribution in eq. (3.21) is left unchanged in the isolated case. As mentioned at the end of section 3, the $\ln R$-dependence of eq. (3.21) exactly cancels the $\ln R$-dependence of eq. (3.19). Since in the isolated case, we have to add eqs. (3.19) and (3.21) and then subtract eq. (5.2), the cancellation of the $\ln R$-dependence does not occur anymore. When $R \ll 1$, the NLO calculation of the isolated cross section is proportional to $\ln 1/R$, and therefore it diverges to $+\infty$ when $R \to 0$.

This divergence is unphysical. Its appearance at NLO simply means that, as soon as R is sufficiently small (see section 6), the NLO calculation is not physically reliable. To improve the reliability of the fixed-order perturbative expansion, higher-order contributions proportional to $(\alpha_s \ln R)^n$ have to be computed when R becomes very small.

Moreover, the calculation in section 3 also tells us that non-perturbative contributions must be taken into account when R is very small. For example, the integral in eq. (3.16) is an integral over the virtuality p_a^2 of the parton a in figure 1. The integral of the perturbative matrix element is performed over the range $0 \le p_a^2 = 2p_q.p_\gamma \le R^2\, p_{T\,\gamma}^2\, (1-z)/z$. However, non-perturbative hadronization effects become dominant as soon as $p_a^2 \le Q_0^2 \sim \mathcal{O}(1\,\mathrm{GeV}^2)$. A strict perturbative treatment of the isolated cross section is thus justified only when

$$R^2\, p_{T\,\gamma}^2\, \frac{1-z}{z} \ge Q_0^2\,. \tag{5.3}$$

If R becomes too small, the perturbative calculation has to be supplemented by a careful treatment of non-perturbative phenomena.

5.2 Fragmentation contribution with isolation

To study the effects of isolation on the fragmentation component, let us consider the subprocess of figure 2, in which a gluon with momentum p_5 is emitted by the quark a that fragments into a photon with momentum p_γ. We denote by p_f the momentum of the collinear hadronic fragments of the quark a. The gluon may or may not belong to the isolation cone around the photon, thus leading to two different restrictions on the allowed kinematics of gluon 5.

i) The gluon is outside the cone. We only have a condition on $p_{T\,f}$

$$p_{T\,f} \le \varepsilon_h\ p_{T\,\gamma}\,. \tag{5.4}$$

Defining

$$p_{T\,a} = p_{T\,f} + p_{T\,\gamma}\,, \qquad z = \frac{p_{T\,\gamma}}{p_{T\,a}}\,, \tag{5.5}$$

we write eq. (5.4) as

$$z \ge z_c\,. \tag{5.6}$$

The variable z is the fragmentation variable appearing in the fragmentation function $D_q^\gamma(z, M_F)$. Going back to expressions (3.6) and (3.8), we see that condition (5.4) restricts the z-integration range. The lower limit now is z_c instead of $z_{\rm min}$ (we are assuming that $z_c > z_{\rm min}$, as is the case in the kinematical configurations of interest in experiments at high-energy colliders).

ii) The gluon belongs to the cone. The isolation criterion (1.1) implies

$$p_{T\,f} + p_{T\,5} \leq \varepsilon_h \, p_{T\,\gamma} \,, \tag{5.7}$$

or, equivalently,

$$p_{T\,a} + p_{T\,5} \leq \frac{p_{T\,\gamma}}{z_c} \,. \tag{5.8}$$

In terms of the variable z in eq. (5.5) and of the variable x,

$$x = \frac{p_{T\,a}}{p_{T\,a} + p_{T\,5}} \,, \tag{5.9}$$

eq. (5.8) is written as

$$z \; x \geq z_c \,. \tag{5.10}$$

The constraint in eq. (5.10) means that, when the gluon is inside the cone, we must also restrict the x-integration range, so that $x \geq z_c/z$ instead of $x \geq z_{\rm min}/z$ has to be used in eq. (3.8).

In summary, we obtain the fragmentation component with isolation by subtracting from the inclusive one the contribution that violates eqs. (5.6) and (5.10). Condition (5.6) is straightforwardly implemented by changing the z-integration range in eqs. (3.6) and (3.8). Condition (5.10) modifies the x-integration range and the function $K_{\rm HO}^{\rm brems}$ in eq. (3.8). Working again within the small-R approximation, we can perform a calculation similar to the one carried out in section 3 in the case of the direct component. We thus obtain the part of the higher-order correction that has to be subtracted from eq. (3.8) (after having implemented the constraint $z > z_c$) when $R \ll 1$:

$$\begin{aligned} d\sigma_{\gamma jet}^{\rm brems,sub} &= 2\pi \left(\frac{\alpha_s(\mu)}{\pi} \right)^3 \sum_{\substack{b \\ a,c=q,\bar{q}}} \int_{z_c}^1 D_a^\gamma(z, M_F) \, dz \, \times \\ &\times \int_{z_{\rm min}/z}^{z_c/z} dx \; C_F \left\{ \ln \left(\frac{R \; p_{T\,\gamma} \; (1-x)}{z \; M_F} \right) \left(\frac{1+x^2}{1-x} \right) + \frac{1}{2}(1-x) \right\} \times \\ &\times E_c \, \frac{d\widehat{\sigma}_{\rm Born}(A+B \to c+b+X)}{d\vec{p}_c \; d\eta_b} \; d\eta_b \; d\eta_c \; p_{T\,c} \; dp_{T\,c} \,. \end{aligned} \tag{5.11}$$

Here the photon momentum is related to the momentum of the parton c by $p_\gamma = zxp_c$. As in the case of the direct component, the explicit R-dependence of the contribution in the curly bracket can be eliminated by choosing the scale $M_F = R \, p_{T\,\gamma}$, at the price of introducing R-dependent effects through the M_F-dependence of the fragmentation function $D_a^\gamma(z, M_F)$.

In the above presentation, we have explicitly considered the subprocess in figure 2, which is collinear- (when $R \to 0$) and infrared- (when $z_c \to 1$) divergent and thus leads to the most important HO corrections. The same approach applies to other subprocesses. For instance, parton a can be a gluon and parton 5 a quark. We obtain corrections similar to those in eq. (5.11), apart from the following replacement. The contribution inside the curly bracket on the right-hand side of eq. (5.11) is:

$$\ln\left(\frac{R\, p_{T\,\gamma}\,(1-x)}{z\, M_F}\right) \widehat{P}^{(4)}_{qq}(x) + \frac{1}{2}\, P^{(n-4)}_{qq}(x)\,, \tag{5.12}$$

where the terms

$$\widehat{P}^{(4)}_{qq}(x) = C_F\,\frac{1+x^2}{1-x}\,, \qquad P^{(n-4)}_{qq}(x) = C_F\,(1-x)\,,$$

build the unregularized Altarelli-Parisi kernel in n dimensions $\widehat{P}^{(n)}_{qq}(x) = \widehat{P}^{(4)}_{qq}(x) - \varepsilon\, P^{(n-4)}_{qq}(x)$. The HO corrections from the subprocess with generic parton species c and a in figure 2 are obtained from eq. (5.11) through the substitution

$$\begin{aligned} \widehat{P}^{(4)}_{qq}(x) &\longrightarrow \widehat{P}^{(4)}_{ac}(x)\,, \\ P^{(n-4)}_{qq}(x) &\longrightarrow P^{(n-4)}_{ac}(x)\,. \end{aligned}$$

The explicit expressions of $\widehat{P}^{(4)}_{ac}(x)$ and $P^{(n-4)}_{ac}(x)$ can be found, for instance, in ref. [35].

The calculation described in this subsection is valid in the limit $R \ll 1$ and thus neglects corrections of $\mathcal{O}(R^{2n})$. These corrections are discussed in section 6.

6. Numerical calculation and $\mathcal{O}(R^{2n})$ terms

The isolation criterion (1.1) modifies the calculation of the HO corrections to prompt-photon production by restricting the available phase space to final-state radiation. In section 5, we have implemented these cuts by working in the collinear approximation for pedagogical purposes. To go beyond the collinear approximation and keep the complete R-dependence of the cross section, we have implemented all the LO and NLO contributions in a computer programme, according to a combined analytical and Monte Carlo approach. In this section we first briefly describe the programme, then we present the results of our numerical study.

6.1 Brief presentation of the programme

The code we use is derived from the NLO Monte Carlo programme DIPHOX [35], designed to calculate the double-inclusive cross sections

$$E\frac{d\sigma(A+B\to F_1+F_2+X)}{d\vec{p}_1\; d\eta_2}$$

and associated distributions, where F_1 and F_2 are large-p_T particles, photons or hadrons [35, 36]. This programme combines the phase-space slicing method [31, 37] and the subtraction method [32, 33] to treat the soft and collinear singular parts of the perturbative matrix elements.

For a generic parton subprocess $1+2\to 3+4+5$, the photon and one outgoing parton, say 3 and 4, have a high p_T and are well separated in phase space, while the remaining final-state parton, say 5, can be either soft or collinear to one of the other four partons. The phase space is sliced by using two arbitrary, unphysical parameters p_{Tm} and R_{Th}, with $p_{Tm} \ll |\vec{p}_{T\,3,4}|$ and $R_{Th} \ll 1$, in the following way:

- Part I corresponds to $|\vec{p}_{T\,5}| < p_{Tm}$. This cylinder supports the soft and initial-state collinear singularities. It also yields a small fraction of the final-state collinear singularities from the subregion in which parton 5 is very soft.

- Part II.a corresponds to the region where $|\vec{p}_{T\,5}| \geq p_{Tm}$ and the parton 5 is inside a cone C_3 about the direction of particle 3, defined by $(y_5-y_3)^2+(\phi_5-\phi_3)^2 \leq R_{th}^2$. This region supports the final-state collinear singularities appearing when 5 is collinear to 3.

- Part II.b is defined in a similar way as II.a, but with the replacement of particle 3 by particle 4. The corresponding cone C_4 supports the final-state collinear singularities appearing when 5 is collinear to 4.

- Part II.c is the remaining region: $|\vec{p}_{T\,5}| \geq p_{Tm}$, and $\vec{p}_{T\,5}$ belongs to neither of the two cones C_3, C_4. This slice yields no divergences, and can thus be treated directly in four space-time dimensions.

Collinear and soft singularities appear in parts I, II.a and II.b. They are first regularized by dimensional continuation from 4 to $n = 4 - 2\varepsilon$ ($\varepsilon < 0$) space-time dimensions. Then, the n-dimensional integration over the kinematic variables (transverse momentum, rapidity and azimuthal angles) of parton 5 is performed analytically over the phase-space regions in I, II.a and II.b. After combination with the corresponding virtual contributions, the soft singularities cancel, and the remaining collinear singularities that do not cancel are factorized and absorbed in the parton distributions and fragmentation functions. The resulting quantities correspond to pseudo cross sections, where the hard partons in the regions I, II.a and II.b are unresolved from the soft or collinear parton 5, which has been "integrated out" inclusively on these parts. The word "pseudo" means that they are not genuine cross sections, as they are not positive-definite in general. These contributions as well as the one from region II.c are then encoded in the Monte Carlo computer programme.

The integration over the phase-space region in II.c, which yields no divergences, is perfomed numerically without any approximation. The implementation of the isolation criterion is straightforward: conditions (5.6) or (5.10) just cut the numerical phase-space integration when parton 5 is outside the isolation cone or inside the annulus $R_{th}^2 \leq (y_5 - y_\gamma)^2 + (\phi_5 - \phi_\gamma)^2 \leq R^2$, respectively.

The region in part I is treated according to the phase-space slicing method. The integration is carried out analytically by neglecting terms that are proportional to powers of p_{Tm} and thus vanish when $p_{Tm} \to 0$. This approximation implies that, when using the numerical programme, the unphysical parameter p_{Tm} has to be chosen sufficiently small for the results to be independent of p_{Tm}. In ref. [35] it was checked that p_{Tm} values of the order of half a per cent of the minimum of p_{T3} and p_{T4} are sufficient.

In principle, the dependence on the unphysical parameter R_{th} can be treated as that on p_{Tm}. However, such a procedure would lead to numerical instabilities when the radius R of the isolation cone is also small. Therefore, to avoid any approximation of the R_{th}-dependence, the integration over the phase-space regions in part II.a and II.b is performed

JHEP05(2002)028

by using the subtraction method. The integrand (i.e. the square of the matrix element) is first replaced by its collinear approximation (see section 3), and the corresponding integration is performed analytically. This calculation is formally identical to the one presented in sections 3 and 5, the isolation-cone radius R now being replaced by the slicing parameter R_{th}. Therefore, after factorization of the collinear singularities in the fragmentation functions, the numerical programme contains expressions like (cf. eq. (5.11))

$$
\begin{aligned}
2\pi \left(\frac{\alpha_s(\mu)}{\pi}\right)^3 \sum_{\substack{b \\ a,c=q,\bar{q}}} \int_{z_{\min}}^1 D_a^\gamma(z, M_F)\; dz \int_{z_{\min}/z}^1 E_c \frac{d\widehat{\sigma}_{\rm Born}(A+B \to b+c+X)}{d\vec{p}_c\; d\eta_b} \times \\
\times\, d\eta_b\; d\eta_c\; p_{T\,c}\; dp_{T\,c} C_F \left\{ \ln\left(\frac{R_{th} p_{T\,c}}{M_F}\right) \left(\frac{1+x^2}{1-x}\right)_+ + (1+x^2)\left(\frac{\ln(1-x)}{1-x}\right)_+ + \right. \\
\left. + \frac{1+x^2}{1-x} \ln x + \frac{1}{2}(1-x) \right\} dx \,,
\end{aligned}
$$

in which the isolation criterion is simply implemented by changing everywhere $z_{\min}$ by z_c. Then, to take into account the exact dependence on R_{th}, the difference between the exact matrix element and its collinear approximation is integrated numerically, yielding finite contributions (which are of $\mathcal{O}(R_{th}^{2n})$ when $R_{th} \to 0$) that are included in the Monte Carlo programme. The results, therefore, do not depend on R_{th}.

In the following we present some numerical studies that implement the isolation criterion in eq. (1.1). However, our NLO Monte Carlo programme can also be used to implement other definitions of isolation, such as, for instance, the isolation criterion in eq. (4.23).

6.2 Numerical results

We start the presentation of our numerical investigations by studying the sensitivity of the cross section with respect to variations of the isolation parameters. We then examine the dependence of the NLO results on the factorization and renormalization scale. We also compare our complete numerical treatment with that in the collinear approximation. Finally, we study the isolated cross section as a function of the transverse momentum of the photon.

6.2.1 Sensitivity to the isolation parameters

We use exact NLO expressions for the isolated cross sections, where "exact" means that the full R-dependence is kept, i.e. all the terms proportional to $R^{2n} (n \geq 1)$ are taken into account on top of the collinear approximation used in section 5. We choose kinematical parameters corresponding to those used by the CDF experiment at Tevatron Run Ib [3]: $\sqrt{S} = 1.8\,\text{TeV}$, $-0.9 \leq y_\gamma \leq 0.9$ and $p_{T\,\gamma} = 15\,\text{GeV}$, which corresponds to the lower range of the photon p_T spectrum. We consider the prompt-photon inclusive cross section

$$
\frac{d\sigma}{dp_{T\,\gamma}} = \int_{y_{\min}}^{y_{\max}} dy\; \frac{d\sigma}{dy_\gamma\; dp_{T\,\gamma}} \,.
$$

Similar studies can be done for photon-jet cross sections [38]. We use the NLO parton distribution functions of the set MRST-99 [39], and the NLO fragmentation functions of set II in Bourhis et al. [23]. The calculations are done with $N_f = 5$ flavours. The renormalization and factorization scales μ and M are both set equal to $p_{T\,\gamma}/2$.

JHEP05(2002)028

Isolation radius	Direct contribution		Fragmentation contribution		Total
R	Born	NLO	Born	NLO	NLO
1.0	1764.6	3318.4	265.0	446.7	3765.1
0.7	1764.6	3603.0	265.0	495.0	4098.0
0.4	1764.6	3968.9	265.0	555.6	4524.5
0.1	1764.6	4758.2	265.0	678.9	5431.1
Without isolation	1764.6	3341.1	1724.3	1876.8	5217.9

Table 1: Isolated cross sections (the values are given in pb/GeV) corresponding to $\varepsilon_h = 0.13333$.

Table 1 shows the sensitivity of the cross section to the value R of the isolation cone. In this study we fixed $\varepsilon_h = 2/15 \simeq 0.13333$, which means that all events with hadronic transverse energy larger than 2 GeV in the isolation cone are rejected. The results without isolation are also reported for comparison. We verify that the Born cross sections are not sensitive to the isolation radius, as they should.

It is interesting to note that the HO contributions, both to the direct and to the fragmentation components, increase when R decreases. This is due to the fact that the implementation of isolation amounts to subtracting a contribution proportional to $\ln R$ from the non-isolated cross section (see eqs. (5.2) and (5.11)). Since this subtracted contribution is negative when $R < 1$, the HO contribution to the direct component of the isolated cross section is quite large for small values of R. A similar behaviour is observed in the HO contribution to the fragmentation component. When all contributions are taken into account, the total cross section (direct + fragmentation) strongly increases with decreasing R.

In particular, when $R = 0.1$, the NLO calculation gives an unphysical result: the isolated cross section turns out to be larger than the non-isolated one! Such a behaviour had to be expected in view of the discussion at the end of section 5.1. The NLO results in table 1 imply that the value $R \sim 0.1$ is sufficiently small to demand the inclusion of beyond-NLO perturbative terms and non-perturbative contributions.

The sensitivity of the cross sections to variations of ε_h is displayed in table 2. Now we fix $R = 0.7$. Note that, already at the Born level, the fragmentation component is quite sensitive to ε_h and strongly decreases when such a cut is installed.

The ratios NLO/Born increase when ε_h decreases, indicating that the effect of higher-order corrections is larger at small than at large ε_h. This is due to the following mechanism. Radiation collinear to the photon is more suppressed by the transverse-energy isolation cut than hard non-collinear radiation. Since the collinear contributions are negative when evaluated in the $\overline{MS}$ factorization scheme (see e.g. eq. (3.19)), their strong suppression leads to a sizeable NLO correction when ε_h decreases. We also note that, as expected, the effect of the ε_h cut-off is very large on the fragmentation component, in which a large part of the z-integration domain is suppressed. The total (direct + fragmentation) cross section at NLO is rather stable with respect to ε_h variations, because of the behaviour of the direct contribution.

Energy cut	Direct contribution		Fragmentation contribution		Total
ε_h	Born	NLO	Born	NLO	NLO
0.03333	1764.6	3820.9	60.3	168.7	3989.6
0.06667	1764.6	3734.3	135.2	303.4	4037.7
0.13333	1764.6	3603.0	265.0	495.0	4098.0
0.33333	1764.6	3434.1	571.2	883.9	4318.0
0.66667	1764.6	3359.5	930.4	1307.5	4667.0
1.00000	1764.6	3340.4	1173.1	1579.4	4919.8

Table 2: Isolated cross sections (the values are given in pb/GeV) corresponding to $R = 0.7$.

Scale	Direct contribution	Fragmentation contribution	Total
	(NLO)	(NLO)	(NLO)
$p_T/2$	3603.0	495.0	4098.0
p_T	3155.3	576.2	3731.5
$2p_T$	2840.7	631.7	3472.4

Table 3: Scale dependence of the isolated cross section in pb/GeV.

We point out that there is no infrared divergence coming from the NLO collinear contribution when $\varepsilon_h \to 0$ ($z_c \to 1$). The direct component contains a term proportional to $\int_{z_c}^1 dz \;\ln(1-z) \simeq (1-z_c)\ln(1-z_c)$ when $z_c \to 1$ (see eqs. (3.19) and (5.2)). The fragmentation component involves terms proportional to $(1-z_c)\ln^3(1-z_c)$: a factor $\ln^2(1-z_c)$ comes from integrating the behaviour $\ln(1-x)/(1-x)$ in eq. (5.11), and a factor $(1-z_c)\ln(1-z_c)$ comes from the convolution with the large-z behaviour, proportional to $\ln(1-z)$, of the NLO fragmentation function $D_q^\gamma(z, M_F)$ [23]. Still in both cases the NLO cross section is finite when $\varepsilon_h \to 0$. However, there are infrared-divergent contributions that are not smoothed out by the convolution with the fragmentation function $D_q^\gamma(z, M_F)$. They correspond to soft gluons emitted non-collinearly to the photon (for instance, emitted from the initial-state quark of the LO direct subprocess $q + \bar{q} \to \gamma + g$) and produce terms proportional to $R^2 \ln \varepsilon_h$ in the direct component of the NLO cross section [11]. The effect of these terms is thus suppressed when the size of the isolation cone is relatively small. The numerical stability of the NLO results in table 3 suggests that the contribution of infrared-divergent terms is not dominant, unless the parameter ε_h becomes very small.

6.2.2 Scale dependence

Until now all calculations have been performed with the renormalization scale μ, the initial-state factorization scale M and final-state fragmentation scale M_F, all equal to $p_{T\,\gamma}/2$. Here we study the sensitivity of the isolated cross section with respect to scale variations. Choosing standard isolation parameters, $\varepsilon_h = 2/15$ and $R = 0.7$, we vary the scale $\mu = M = M_F$ between $p_{T\,\gamma}/2$ and $2p_{T\,\gamma}$. The results are given in table 3. They can be compared with the corresponding results obtained without isolation, which are displayed in table 4.

Scale	Direct contribution	Fragmentation contribution	Total
	(NLO)	(NLO)	(NLO)
$p_T/2$	3341.1	1876.8	5217.9
p_T	2643.7	2122.6	4766.3
$2p_T$	2188.8	2250.7	4439.5

Table 4: Scale dependence of the non-isolated cross section in pb/GeV.

R	$\varepsilon_h = 2/30 \simeq 0.06667$		$\varepsilon_h = 2/15 \simeq 0.13333$	
	Small-cone approx.	No approx.	Small-cone approx.	No approx.
1.0	292.5	267.7	482.4	446.7
.7	313.7	303.4	512.8	495.0
.4	344.0	345.6	560.9	555.6
.1	431.8	432.9	678.9	678.9

Table 5: Comparison between our results (no approximation) and the small-cone approximation [11] for the fragmentation component. The cross sections are given in pb/GeV.

The cross section decreases monotonically in both cases when the scale increases. The magnitude of the effect is comparable in the two cases: a relative variation of the cross section by $\sim$ 16% is observed in the range of scales considered. We conclude that the implementation of isolation does not induce any extra sensitivity to the scale arbitrariness, at least when the three scales μ, M, M_F are kept equal.

6.2.3 Comparison with the collinear approximation

The isolation criterion used in ref. [11] is based on an upper limit on the hadronic c.m. energy rather than on the hadronic transverse energy inside the isolation cone. As pointed out in ref. [11] and discussed in general terms in section 4, in the case of soft and collinear parton radiation, the two variants of the isolation criterion become equivalent by simply identifying the c.m.-energy parameter ε of ref. [11] with our transverse-energy parameter ε_h in eq. (4.16). Since the approximate NLO calculation performed in ref. [11] is actually based on the soft and collinear limits, it can thus be compared with our calculation by setting $\varepsilon_h = \varepsilon$.

More precisely, the authors of ref. [11] derived approximate analytical expressions for the NLO terms $\sigma_{\rm HO}^{\rm is}$ in eqs. (4.18) and (4.19). These expressions are valid in the small-cone[3] approximation $R \ll 1$, and thus neglect corrections that are of $\mathcal{O}(R^2)$ when $R \to 0$. In this limit the collinear approximation is valid, and our results in eqs. (5.2) and (5.11) fully agree with those in ref. [11]. In the case of the direct contribution $\sigma_{\rm HO}^{\gamma,{\rm is}}$, the authors of ref. [11] also computed the dominant correction due to soft-gluon emission. This correction behaves as $R^2 \ln \varepsilon_h$ when $\varepsilon_h \to 0$ and $R \ll 1$.

[3] In ref. [11] the cone size δ is defined with respect to the relative angles in the c.m. frame. When $R \ll 1$, we thus have $R = \delta \cosh \eta_\gamma$.

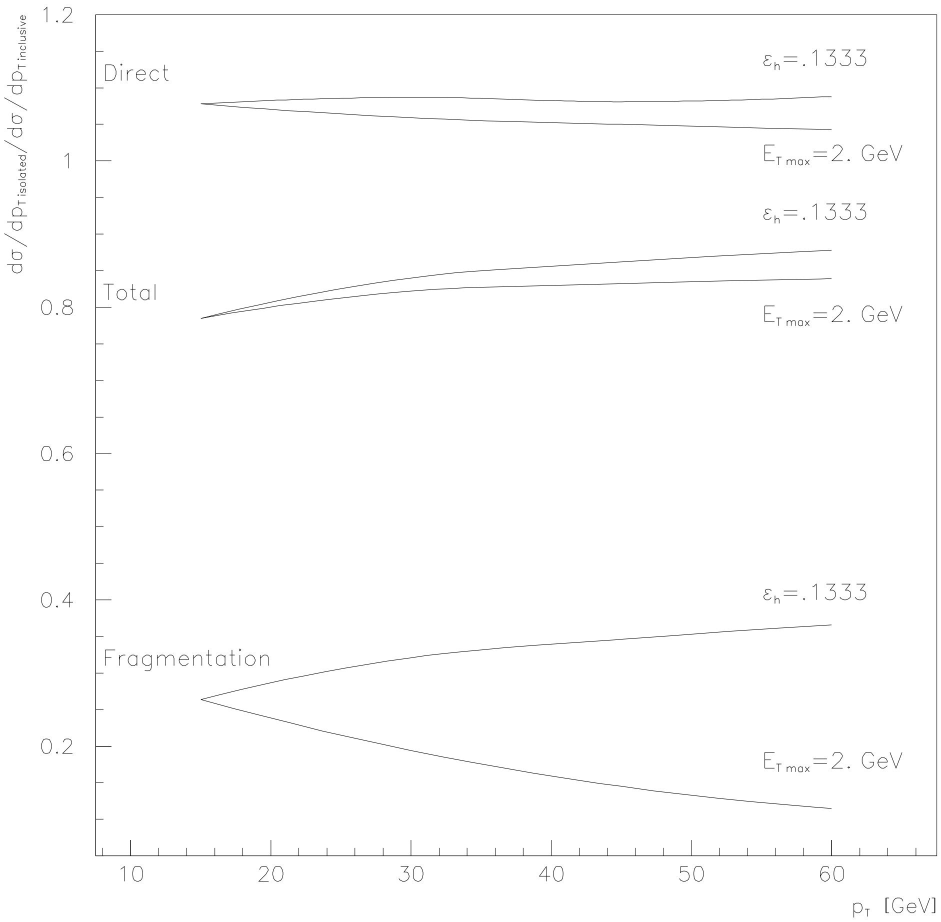

Figure 3: Ratios "isolated"/"non-isolated" for the direct contribution, the fragmentation contribution and the total contribution to the cross section $d\sigma/dp_{T\,\gamma}$ at NLO.

In the case of the fragmentation component, table 5 shows a comparison between our NLO calculation and that of ref. [11]. We see that there is a good agreement between the two calculations when $R \ll 1$, the collinear approximation becoming more accurate as R decreases (our results are obtained by Monte Carlo integration with an accuracy of 1%). For large values of $R \sim 1$, the small-cone approximation overestimates the fragmentation contribution to the isolated cross section by about 8%. In the case of the direct component, similar results were found in ref. [11] by a numerical comparison with the calculation performed by a Monte Carlo code.

6.2.4 Effect of the isolation as a function of $p_{T\,\gamma}$

Finally we study the effect of isolation as a function of $p_{T\,\gamma}$. Figure 3 shows the ratios "isolated"/"non-isolated" of the direct contributions, the fragmentation contributions, and the total contributions to the NLO cross sections $d\sigma/dp_{T\,\gamma}$. The ratios are displayed in the range $15\,\mathrm{GeV} \leq p_{T\,\gamma} \leq 60\,\mathrm{GeV}$, for two different choices of isolation parameters, both with an isolation cone of radius $R = 0.7$:

one with a fixed value of $E_{T\,\max} = 2\,\mathrm{GeV}$,

one with a fixed value of $\varepsilon_h = E_{T\,\max}/p_{T\,\gamma} = 2/15 \simeq 0.1333$,

which coincide when $p_{T\,\gamma} = 15\,\mathrm{GeV}$.

As for the fragmentation component, isolation using a fixed $E_{T\,\max}$ acts more and more severely as $p_{T\,\gamma}$ increases, while by fixing ε_h the amount of accompanying transverse energy in the cone increases with $p_{T\,\gamma}$. Therefore the ratios "isolated"/"non-isolated" with fixed $E_{T\,\max}$ and with fixed ε_h have opposite variations when $p_{T\,\gamma}$ varies.

Isolation has a rather small effect on the direct contribution in both cases, since it does not act at the Born level.

The effect of isolation on the total contribution to the NLO cross section slightly decreases as $p_{T\,\gamma}$ increases, but it actually depends only weakly on $p_{T\,\gamma}$.

7. Conclusions and outlook

7.1 Conclusions

In this paper we have considered the production of isolated photons in hadronic collisions. We have shown that isolation does not spoil the factorization properties that are valid in the case of inclusive production, and we have discussed the general factorized structure of the isolated-photon cross section. We have then performed a detailed NLO study of the implementation of the isolation criterion in the direct and fragmentation components of the production cross section. For pedagogical purposes, we have first given analytic expressions of the isolated cross sections obtained by using the collinear approximation, i.e. valid in the limit of small radius R of the isolation cone. To go beyond the collinear approximation, we have implemented the isolation criterion in a computer programme that encodes the exact dependence of the cross section on the cone radius at NLO accuracy.

The main result of our NLO numerical study is that the inclusive cross section for isolated photons has a magnitude comparable to the one for non-isolated photons. Each separate component, direct and fragmentation, sizeably depends on the isolation parameters, both at LO and NLO. However, the measurable cross section, given by the sum "direct + fragmentation", does not vary by more than 10% when ε_h varies between $2/30 \simeq 0.06667$ and 0.333, or when R varies between 0.4 and 0.7. Nonetheless, with small cones such as $R \sim 0.1$, the result of the NLO calculation for the isolated cross section becomes larger than the one in the non-isolated case. This counterintuitive and unphysical result reflects the fact that the fixed-order perturbative calculation is no longer reliable when R is very small: when $\alpha_s \ln 1/R^2 \sim 1$, perturbative contributions beyond the NLO have to be taken into account; when $R\,p_{T\,\gamma} \sim \mathcal{O}(1\,\mathrm{GeV})$, also non-perturbative contributions are demanded. The scale dependence of the cross sections is similar in the isolated and non-isolated cases: the cross sections decrease monotonically by $\sim 16\%$ when the common scale $\mu = M = M_F$ varies between $p_T/2$ and $2p_T$. Comparing our NLO calculation with its small-cone approximation [11], we find that the latter is adequate at small R and overestimates the cross section by about 8 to 10% at large R values, $R \sim 1$. Finally, isolation is found to weakly affect the $p_{T\gamma}$-dependence of the cross section $d\sigma/dp_{T\,\gamma}$ in the range $15\,\mathrm{GeV} \leq p_{T\,\gamma} \leq 60\,\mathrm{GeV}$.

7.2 Open problems

We conclude with some remarks on several questions left open by our NLO treatment when the cone radius R becomes too small, as well as when the parameter $E_{T\,\max}$ is small and isolation becomes very tight.

7.2.1 Small cone radius

As seen numerically in section 6, the result of the NLO calculation for the isolated cross section at $p_{T\gamma} = 15\,\mathrm{GeV}$ violates the physical constraint $\sigma(\text{with isol.}) < \sigma(\text{no isol.})$ when $R \sim 0.1$. This value of R is smaller than the ones relevant to experimental practice. However, the value $R \sim 0.1$ is not much smaller than the value $R = 0.4$ that is used in the most recent measurements at the Tevatron [4, 5] and that is going to be used at the LHC [14]. Therefore, we should be concerned about the actual value of R below which the reliability of the fixed-order perturbative calculation breaks down.

Note that $p_{T\gamma} = 15\,\mathrm{GeV}$ and $R = 0.1$ imply $R\,p_{T\gamma} \sim 1\,\mathrm{GeV}$ and $\alpha_s(\mu^2)\ln 1/R^2 \sim 1$ (recall that $\mu = p_{T\gamma}/2$ is used in the numerical results of table 1). Therefore, as discussed at the end of section 5.1, the scale $R\,p_{T\gamma}$ is close to the non-perturbative region and, at the same time, higher-order corrections proportional to $(\alpha_s \ln 1/R^2)^n$ can be relevant. Summation of the logarithmic dependence on R to all perturbative orders, combined with a careful study of the border-line between perturbative and non-perturbative regions, has to be undertaken to improve our understanding of the small-R behaviour of isolated-photon prodution. Work in this direction is in progress, and the results will be reported elsewhere.

7.2.2 Tight isolation

Formally, the perturbative calculation of the cross section of isolated prompt photons is infrared-divergent in the limit $\varepsilon_h \to 0$. Indeed, $\varepsilon_h = 0$ would imply that the isolation cone about the photon would become an absolutely forbidden region of the phase space for gluon radiation, no matter how soft it is, thus spoiling the cancellation of infrared singularities between real and virtual soft-gluon contributions. As discussed in section 6, at NLO this divergent behaviour shows up as a logarithmic term proportional to $\alpha_s R^2 \ln \varepsilon_h$ in the direct component of the cross section.

In practice, using a cone of radius $R = 0.7$, we have found no significant infrared sensitivity in our numerical study, down to the very low value $\varepsilon_h = 0.033333$, which corresponds to $E_{T\,\max} = 0.5\,\mathrm{GeV}$ for a photon with $p_{T\gamma} = 15\,\mathrm{GeV}$. Therefore the implementation of the isolation criterion (1.1) with (finite but) tight transverse-energy cuts does not seem to destabilize the numerical convergence of the perturbative expansion. Nonetheless, owing to the presence of higher powers of $\ln \varepsilon_h$ at higher perturbative orders, the actual sensitivity of the cross section to very low values of ε_h is probably underestimated in the present NLO calculation.

In the present work we have treated all the quarks as being massless. This treatment is not adequate in the case of a heavy quark when $E_{T\,\max}$ is comparable to its mass. This issue especially concerns heavy quarks that are experimentally not identified. In this case, better theoretical calculations and studies of heavy-quark fragmentation based on Monte Carlo event generators are required.

JHEP05(2002)028

In the NLO calculation, isolation is implemented at the parton level. In an actual event, a fraction of the hadronic transverse energy that accompanies a photon to be selected by the criterion (1.1) comes also from the low-p_T underlying event, as well as from pile-up effects in collisions at very high luminosity. Part of these effects can be mimicked in the NLO calculation by using an effective value of $E_{T\,\max}$ that is lower than that imposed at the detector level. However, this procedure does not take into account the fact that the underlying event causes also some suppression of the direct component at the Born level, which is independent of $E_{T\,\max}$. Model estimates [40] of this suppression indicate that it can be quantitatively relevant when the value of $E_{T\,\max}$ at the detector level is small. In general, as the isolation becomes tight, the perturbative calculation has to be supplemented by careful studies of the effects of the underlying event and pile-up.

Acknowledgments

We thank Werner Vogelsang for sending us his numerical results. We also thank Stefano Frixione and Bryan Webber for discussions. This work was supported in part by the EU Fourth Training Programme "Training and Mobility of Researchers", Network "Quantum Chromodynamics and the Deep Structure of Elementary Particles", Contract FMRX-CT98-0194 (DG 12 - MIHT). LPT is a "Unité Mixte de Recherche du CNRS (UMR 8627) associée à l'Université de Paris XI". LAPTH is a "Unité Mixte de Recherche du CNRS (UMR 5108) associée à l'Université de Savoie".

References

[1] UA1 collaboration, C. Albajar et al., *Direct photon production at the Cern $\bar{p}p$ collider*, *Phys. Lett.* **B 209** (1988) 385; *Low mass dimuon production at the Cern $\bar{p}p$ collider*, *Phys. Lett.* **B 209** (1988) 397.

[2] UA2 collaboration, J.A. Appel et al., *Direct photon production at the Cern $\bar{p}p$ collider*, *Phys. Lett.* **B 176** (1986) 239; *Direct photon production in $\bar{p}p$ collisions at $\sqrt{s} = 630$ GeV* *Z. Physik* **C 41** (1988) 395;
UA2 collaboration, J. Alitti et al., *A Measurement of the direct photon production cross-section at the CERN $\bar{p}p$ collider*, *Phys. Lett.* **B 263** (1991) 544; *A measurement of single and double prompt photon production at the CERN $\bar{p}p$ collider*, *Phys. Lett.* **B 288** (1992) 386.

[3] CDF collaboration, F. Abe et al., *Measurement of the isolated prompt photon cross-sections in $\bar{p}p$ collisions at $\sqrt{s} = 1.8$ TeV*, *Phys. Rev. Lett.* **68** (1992) 2734;
A prompt photon cross-section measurement in $\bar{p}p$ collisions at $\sqrt{s} = 1.8$ TeV, *Phys. Rev.* **D 48** (1993) 2998;
A precision measurement of the prompt photon cross-section in $p\bar{p}$ collisions at $\sqrt{s} = 1.8$ TeV, *Phys. Rev. Lett.* **73** (1994) 2662.

[4] D0 collaboration, S. Abachi et al., *Isolated photon cross-section in the central and forward rapidity regions in $p\bar{p}$ collisions at $\sqrt{s} = 1.8$ TeV*, *Phys. Rev. Lett.* **77** (1996) 5011 [hep-ex/9603006];
D0 collaboration, B. Abbot et al., *The isolated photon cross-section in $p\bar{p}$ collisions at $\sqrt{s} = 1.8$ TeV*, *Phys. Rev. Lett.* **84** (2000) 2786;

D0 collaboration, V.M. Abazov et al., *The ratio of the isolated photon cross sections at $\sqrt{s} = 630\,GeV$ and 1800 GeV*, *Phys. Rev. Lett.* **87** (2001) 251805 [hep-ex/0106026].

[5] CDF collaboration, D. Acosta et al., *Comparison of the isolated direct photon cross sections in $p\bar{p}$ collisions at $\sqrt{s} = 1.8\,TeV$ and $\sqrt{s} = 0.63\,TeV$*, hep-ex/0201004.

[6] ZEUS collaboration, J. Breitweg et al., *Measurement of inclusive prompt photon photoproduction at Hera*, *Phys. Lett.* **B 472** (2000) 175 [hep-ex/9910045].

[7] P. Aurenche, R. Baier, M. Fontannaz and D. Schiff, *Prompt photon production at large p_T scheme invariant QCD predictions and comparison with experiment*, *Nucl. Phys.* **B 297** (1988) 661.

[8] P. Aurenche, R. Baier and M. Fontannaz, *Prompt photon production at colliders*, *Phys. Rev.* **D 42** (1990) 1440.

[9] H. Baer, J. Ohnemus and J.F. Owens, *A next-to-leading logarithm calculation of direct photon production*, *Phys. Rev.* **D 42** (1990) 61.

[10] E.L. Berger and J. Qiu, *Calculations of prompt photon production in QCD*, *Phys. Rev.* **D 44** (1991) 2002.

[11] L.E. Gordon and W. Vogelsang, *Polarized and unpolarized isolated prompt photon production beyond the leading order*, *Phys. Rev.* **D 50** (1994) 1901.

[12] W. Vogelsang and A. Vogt, *Constraints on the proton's gluon distribution from prompt photon production*, *Nucl. Phys.* **B 453** (1995) 334 [hep-ph/9505404].

[13] P. Aurenche, R. Baier, M. Fontannaz, J.F. Owens and M. Werlen, *The gluon contents of the nucleon probed with real and virtual photons*, *Phys. Rev.* **D 39** (1989) 3275.

[14] CMS collaboration, *Technical proposal*, report CERN/LHCC/94-38 (1994);
ATLAS collaboration, *ATLAS detector and physics performance: technical design report*, volume 2, report CERN/LHCC/99-15 (1999).

[15] S. Frixione, *Isolated photons in perturbative QCD*, *Phys. Lett.* **B 429** (1998) 369 [hep-ph/9801442].

[16] S. Frixione and W. Vogelsang, *Isolated photon production in polarized pp collisions*, *Nucl. Phys.* **B 568** (2000) 60 [hep-ph/9908387].

[17] S. Catani et al., *QCD*, in *Proceedings of the CERN Workshop on Standard Model Physics (and more) at the LHC*, G. Altarelli and M.L. Mangano eds., CERN 2000-04, Geneva, 2000, p. 1 [hep-ph/0005025].

[18] Z. Kunszt and Z. Trócsányi, *QCD corrections to photon production in association with hadrons in e^+e^- annihilation*, *Nucl. Phys.* **B 394** (1993) 139 [hep-ph/9207232].

[19] E.L. Berger, X.-F. Guo and J.-W. Qiu, *Breakdown of conventional factorization for isolated photon cross sections*, *Phys. Rev. Lett.* **76** (1996) 2234 [hep-ph/9512281]; *Isolated prompt photon production in hadronic final states of e^+e^- annihilation*, *Phys. Rev.* **D 54** (1996) 5470 [hep-ph/9605324].

[20] P. Aurenche, M. Fontannaz, J.P. Guillet, A. Kotikov and E. Pilon, *Is factorization for isolated photon cross sections broken?*, *Phys. Rev.* **D 55** (1997) 1124 [hep-ph/9606287].

[21] S. Catani, M. Fontannaz and E. Pilon, *Factorization and soft-gluon divergences in isolated-photon cross sections*, *Phys. Rev.* **D 58** (1998) 094025 [hep-ph/9803475].

JHEP05(2002)028

[22] E.W.N. Glover and A.G. Morgan, *Measuring the photon fragmentation function at Lep*, *Z. Physik* **C 62** (1994) 311.

[23] L. Bourhis, M. Fontannaz and J.P. Guillet, *Quark and gluon fragmentation functions into photons*, *Eur. Phys. J.* **C 2** (1998) 529 [hep-ph/9704447].

[24] F. Aversa, P. Chiappetta, M. Greco and J.P. Guillet, *Higher order corrections to QCD jets*, *Phys. Lett.* **B 210** (1988) 225; *Higher order corrections to QCD jets: gluon-gluon processes*, *Phys. Lett.* **B 211** (1988) 465; *QCD corrections to parton-parton scattering processes*, *Nucl. Phys.* **B 327** (1989) 105.

[25] E. Laenen, G. Oderda and G. Sterman, *Resummation of threshold corrections for single-particle inclusive cross sections*, *Phys. Lett.* **B 438** (1998) 173 [hep-ph/9806467].

[26] S. Catani, M.L. Mangano and P. Nason, *Sudakov resummation for prompt-photon production in hadron collisions*, *J. High Energy Phys.* **07** (1998) 024 [hep-ph/9806484].

[27] S. Catani, M.L. Mangano, P. Nason, C. Oleari and W. Vogelsang, *Sudakov resummation effects in prompt photon hadroproduction*, *J. High Energy Phys.* **03** (1999) 025 [hep-ph/9903436].

[28] N. Kidonakis and J.F. Owens, *Soft-gluon resummation and NNLO corrections for direct photon production*, *Phys. Rev.* **D 61** (2000) 094004 [hep-ph/9912388].

[29] G. Sterman and W. Vogelsang, *Threshold resummation and rapidity dependence*, *J. High Energy Phys.* **02** (2001) 016 [hep-ph/0011289].

[30] E. Laenen, G. Sterman and W. Vogelsang, *Recoil and threshold corrections in short-distance cross sections*, *Phys. Rev.* **D 63** (2001) 114018 [hep-ph/0010080].

[31] W.T. Giele and E.W.N. Glover, *Higher order corrections to jet cross-sections in e^+e^- annihilation*, *Phys. Rev.* **D 46** (1992) 1980;
W.T. Giele, E.W.N. Glover and D.A. Kosower, *Higher order corrections to jet cross-sections in hadron colliders*, *Nucl. Phys.* **B 403** (1993) 633 [hep-ph/9302225].

[32] R.K. Ellis, D.A. Ross and A.E. Terrano, *The perturbative calculation of jet structure in e^+e^- annihilation*, *Nucl. Phys.* **B 178** (1981) 421;
Z. Kunszt and D.E. Soper, *Calculation of jet cross-sections in hadron collisions at order α_s^3*, *Phys. Rev.* **D 46** (1992) 192;
S. Frixione, Z. Kunszt and A. Signer, *Three-jet cross sections to next-to-leading order*, *Nucl. Phys.* **B 467** (1996) 399 [hep-ph/9512328].

[33] S. Catani and M.H. Seymour, *The dipole formalism for the calculation of QCD jet cross sections at next-to-leading order*, *Phys. Lett.* **B 378** (1996) 287 [hep-ph/9602277]; *A general algorithm for calculating jet cross sections in NLO QCD*, *Nucl. Phys.* **B 485** (1997) 291 [hep-ph/9605323], erratum *ibid.* **B 510** (1998) 503.

[34] S. Catani and B.R. Webber, *Infrared safe but infinite: soft-gluon divergences inside the physical region*, *J. High Energy Phys.* **10** (1997) 005 [hep-ph/9710333].

[35] T. Binoth, J.P. Guillet, E. Pilon and M. Werlen, *A full next to leading order study of direct photon pair production in hadronic collisions*, *Eur. Phys. J.* **C 16** (2000) 311 [hep-ph/9911340].

[36] P. Chiappetta, R. Fergani and J.P. Guillet, *Production of two large p_T hadrons from hadronic collisions*, *Z. Physik* **C 69** (1996) 443.

JHEP05(2002)028

[37] M. Furman, *Study of a nonleading QCD correction to hadron calorimeter reactions*, *Nucl. Phys.* **B 197** (1982) 413.

[38] M. Fontannaz, J.P. Guillet and E. Pilon, work in preparation.

[39] A.D. Martin, R.G. Roberts, W.J. Stirling and R.S. Thorne, *Parton distributions and the LHC: W and Z production*, *Eur. Phys. J.* **C 14** (2000) 133 [hep-ph/9907231].

[40] M. Fontannaz, J.P. Guillet and G. Heinrich, *Isolated prompt photon photoproduction at NLO*, *Eur. Phys. J.* **C 21** (2001) 303 [hep-ph/0105121].